Available online at www.sciencedirect.com

SCIENCE DIRECT®

Lithos 78 (2004) 389–409

LITHOS

www.elsevier.com/locate/lithos

Comprehensive chemical analyses of natural cordierites: implications for exchange mechanisms

Christian Bertoldi[a,b,*], Alexander Proyer[c], Dieter Garbe-Schönberg[a], Harald Behrens[d], Edgar Dachs[b]

[a]*Institut für Geowissenschaften, Universität Kiel, Ludewig-Meyn-Str. 10, 24118 Kiel, Germany*
[b]*Abteilung für Mineralogie und Materialwissenschaften, Universität Salzburg, Hellbrunnerstraße 34, A-5020 Salzburg, Austria*
[c]*Institut für Mineralogie und Petrologie, Universität Graz, Universitätsplatz 2/II, A-8010 Graz, Austria*
[d]*Institut für Mineralogie, Universität Hannover, Callinstraße 3, D-30167 Hannover, Germany*

Received 22 January 2004; accepted 30 July 2004
Available online 5 October 2004

Abstract

Cordierite samples from pegmatites and metamorphic rocks have been analysed for major [electron microprobe analysis (EMPA)] and trace elements [inductively coupled plasma mass spectrometry (ICP-MS), secondary ion mass spectrometry analyses (SIMS)] as well as for H_2O and CO_2 (coulometric titration), and the results evaluated in conjunction with published data in order to determine which exchange mechanisms are significant. Apart from the homovalent substitutions $FeMg_{-1}$ and $MnMg_{-1}$ on the octahedral site, some minor KNa_{-1} on the Ch0 channel site, and $Fe^{3+}Al_{-1}$ on the T_11 tetrahedral site, the three most important substitution mechanisms are those for the incorporation of Li on the octahedral sites ($NaLi\square_{-1}Mg_{-1}$), and of Be and other divalent cations on the tetrahedral T_11 site ($NaBe\square_{-1}Al_{-1}$ and $Na(Mg,Fe^{2+})\square_{-1}Al_{-1}$). The dominant role of the last vector is clearly demonstrated. We propose a new generalized formula for cordierite: $^{Ch}(Na,K)_{0-1}$ $^{VI}(Mg,Fe^{2+},Mn,Li)_2$ $^{IV}Si_5$ $^{IV}Al_3$ $^{IV}(Al, Be, Mg, Fe^{2+}, Fe^{3+})O_{18}$ $*x^{Ch}(H_2O, CO_2\ldots)$. Our results show that the population of (Mg, Fe^{2+}) on the T_11-site is limited to about 0.08 a.p.f.u. Other exchange mechanisms that were encountered in experiments operate only under *P–T* conditions or in bulk compositions that are rarely realized in nature. Routine analyses by electron microprobe in which Li and Be are not determined can be plotted as (Mg+Fe+Mn) versus (Si+Al) to assess whether significant amounts of Li and Be could be present. These amounts can be calculated as Li (a.p.f.u.)=Al+Na–4 and Be (a.p.f.u.)=10–2Al–M^{2+}–Na.
© 2004 Elsevier B.V. All rights reserved.

Keywords: Cordierite; Lithium; Beryllium; Exchange mechanisms

1. Introduction

The mineral cordierite is an important and common rock forming mineral in medium and high-grade aluminous rocks of the amphibolite and granulite

* Corresponding author. Tel.: +43 662 8044 5407.
E-mail address: christian.bertoldi@sbg.ac.at (C. Bertoldi).

0024-4937/$ - see front matter © 2004 Elsevier B.V. All rights reserved.
doi:10.1016/j.lithos.2004.07.003

facies. The two main reasons that cordierite has attracted a lot of attention during the last 50 years are (1) its usefulness as a thermobarometer based on Fe–Mg exchange with garnet and (2) order–disorder and cell size. There has been considerable interest in the distortion index Δ, which is a measure of deviation from the geometrically hexagonal unit cell, and in the ability of cordierite to incorporate variable amounts of uncharged molecules, such as H_2O and CO_2, in its channels and to serve as a potential recorder of paleofluid composition. It has, however, been known for some time that the light elements Li and Be can be highly enriched in cordierite (up to 4139 ppm Li_2O and up to 6378 ppm BeO), which affects formula recalculation and contributes to the fact that electron microprobe totals are often less than 100%. Most of the published cordierite analyses do not report Li or Be contents (see Appendix A for a summary of those that do). In addition, the analytical accuracy and precision available to these authors for major and trace elements has often remained insufficient to isolate beyond doubt all exchange vectors contributing to measured cordierite compositions.

We therefore decided to perform chemical analyses by electron microprobe analysis (EMPA), by inductively coupled plasma mass spectrometry (ICP-MS) and by coulorimetric titration for H_2O and CO_2 with as much care as possible in order to obtain complete, highly accurate and precise analyses of cordierites, and to constrain the most relevant substitution vectors controlling the composition of cordierites from a wide range of parageneses.

1.1. Crystal chemistry and trace element fractionation

Cordierites with the idealized composition $(Mg,Fe)_2[Al_4Si_5O_{18}]*(H_2O,CO_2)$ are silicates with a tetrahedral framework structure and occur in nature mostly in the (Si,Al)-ordered orthorhombic low-temperature modification. Indialite or high-cordierite, the (Si,Al)-disordered hexagonal high temperature modification, is very rare in nature. In low-cordierite different types of tetrahedral and channel sites are distinguished: $(M)_2(T_11)_2(T_26)_2(T_23)_2(T_21)_2(T_16)O_{18}$, (Ch0, Ch1/4). Six-membered rings of T_2 tetrahedra are cross-linked into a framework by T_1 tetrahedra (Fig. 1). The octahedral M-sites typically contain Mg^{2+}, Fe^{2+}, Mn^{2+} as well as Li^+. Al is ordered on T_11 and T_26, whereas Si occupies T_16, T_21 and T_23. Be and small amounts of Mg^{2+}, Fe^{2+} and Fe^{3+} can enter the distorted T_11-site. Open channels parallel to [001]

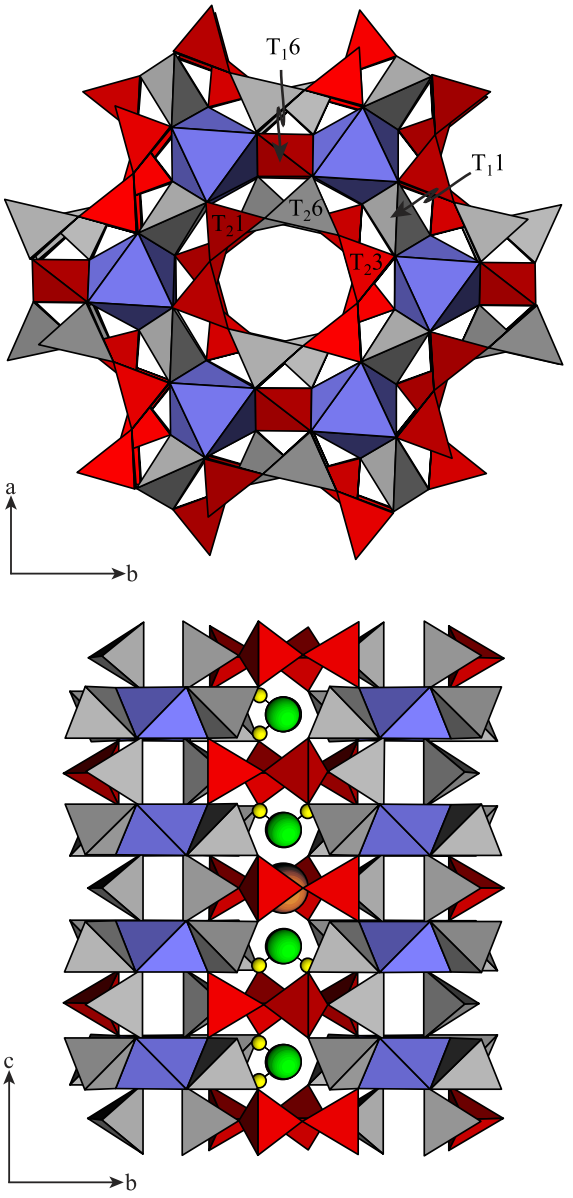

Fig. 1. Polyhedral structural model of low cordierite. Si occupies the tetrahedra in red (T_16, T_21 and T_23) and Al those in grey (T_11 and T_26). The large brown sphere represents sodium in the Ch0-site. The small yellow spheres connected to a green sphere represent a water molecule in the Ch1/4-site with its H–H vector parallel (Type I) or perpendicular (Type II) to [001] (Goldman et al., 1977). (For interpretation of the references to colour in this figure legend, the reader is referred to the web version of this article.)

range in diameter from ~2.6 Å (Ch0-site) to 5.4 Å along b and to 6.0 Å along a (Ch1/4-site). Na^+ or K^+ (and rarely Cs^+ and Ca^{2+}) ions can occupy Ch0, whereas molecules such as H_2O and CO_2 can be incorporated on Ch1/4 (Gibbs, 1966; Meagher, 1967; Cohen et al., 1977; Meagher and Gibbs, 1977; Hochella et al., 1979; Wallace and Wenk, 1980; Vance and Price, 1984; Armbruster, 1985b; Armbruster, 1986; Geiger et al., 2000a,b; Malcherek et al., 2001). Mass spectrometer investigations disclosed minor amounts of other gases, which are released from cordierite during heating: CO, N_2, H_2, O_2, He, Ne, Ar, CH_4, H_2S (Damon and Kulp, 1958; Beltrame et al., 1976; Heide, pers. comm.).

Intervalence charge transfer between the Fe^{2+} in the octahedron and Fe^{3+} in the edge shared $T_1$1 tetrahedron causes colour and pleochroism in cordierite (Faye et al., 1968; Robbins and Sterns, 1968; Pollack, 1976; Smith and Strens, 1976; Parkin et al., 1977; Vance and Price, 1984). Recent Mössbauer investigations on cordierites showed that the amount of Fe^{3+} on the $T_1$1-site in natural cordierites, no matter whether Mg-rich or Fe-rich, is generally low, i.e., below 0.004 a.p.f.u. Fe^{3+} (Černý et al., 1997; Geiger et al., 2000b).

Cordierite was investigated for trace elements by Beeson (1978), Giraud et al. (1986), Harris et al. (1992), Bea et al. (1994, 1996), Bea (1996) and Bea and Montero (1999), who showed that cordierite strongly fractionates Li and Be, whilst the concentrations of the REEs Y, Th and U are very low. The most important elements proved to be Li, Be, Cs and Mn.

Most of the Na–Be-cordierites with more than 0.1 wt.% BeO have been found in pegmatites (unmetamorphosed and metamorphosed) and in related vein deposits (Grew, 2002; Černý, 2002), whereas the Be-cordierite of Alpe Sponda occurs in a kyanite–paragonite–staurolite schist and is strictly metamorphic with no evidence for the introduction of Be from an external source (Armbruster and Irouschek, 1983). Grew (2002) stated that cordierite, like sapphirine and kornerupine–prismatine, is a sink for Be, and proposed that the sequence of fractionation between the sinks is most likely sapphirine–kornerupine–prismatine>cordierite. Based on LA-ICP-MS analyses of minerals from the upper-amphibolite and granulite facies of Peña Negra, Spain (Bea et al., 1994), and Ivrea-Verbano, Italy (Bea and Montero, 1999), Grew (2002) derived the following sequence for the incorporation of Be: cordierite ⩾ whole-rock–sillimanite–biotite–garnet>plagioclase>K-feldspar.

Cordierites in which Li dominates over Be are reported from pegmatites in Dolní Bory, Czech Republic (Černý et al., 1997; Armbruster and Irouschek, 1983; Malcherek et al., 2001), from contact metamorphic schists in Kos, Greece (Kalt et al., 1998), from migmatites of the Peña Negra Complex, Spain (Bea et al., 1994; Malcherek et al., 2001), from biotite schists and leucocratic kyanite bearing gneisses in Miregn, Switzerland (Armbruster and Irouschek, 1983), and from a pelitic schist with a garnet–cordierite–sillimanite–quartz assemblage in south-central Maine, USA (Ferry, 1980; Armbruster, 1986). Cordierites can be a sink for Li if the Na activity is high, even if Li concentration is very low in the parent medium (Černý et al., 1997). The sequence of Li fractionation into common metapelitic minerals is in the order: staurolite>cordierite>biotite>muscovite>garnet, tourmaline, and chloritoid (Dutrow et al., 1986). For comparison, Steppan (2003) found the following sequence of Li and Be fractionation in cordierite-free metapelites: staurolite>biotite>chlorite>muscovite>garnet>tourmaline>andalusite>plagioklase>kyanite for Li, and staurolite>plagioclase>muscovite>biotite>tourmaline>chlorite>kyanite>garnet>andalusite for Be.

Boron, another light element that is not detected in routine electron microprobe analyses, does not enter cordierite in significant amounts, most likely because of “B–Al” avoidance (Klaska and Grew, 1991).

Cordierite is the only magmatic mineral in granitic rocks in which Cs behaves compatibly and is expected to enter the channels (Evans et al., 1980, Schreyer et al., 1990; London, 1995; Thompson et al., 2002; Evensen and London, 2003). The presence or absence of cordierite may largely determine the budget of Be in granitic rocks (London and Evensen, 2002). According to Evensen and London (2002), the distribution of Be and Cs in granitic magmas is controlled by cordierite, that of Li by micas, and that of Mn by biotite and cordierite.

Indialite or high cordierite (P6/mcc) is found in pyrometamorphic meltrocks or paralavas (which are rocks melted by proximity to burning coal seams), in buchites (Fermor, 1924; Venkatesh, 1952; Miya-

shiro and Iiyama, 1954; Schreyer et al., 1990; Sokol et al., 1998) and in volcanic xenoliths (Hentschel, 1977; Schreyer et al., 1990). Potassic cordierites with up to 1.71 wt.% K_2O are either hexagonal high-cordierites or preserve intermediate structural states. They occur in typical high-temperature/very low pressure sanidine facies environments showing evidence of rapid growth as well as rapid cooling (Schreyer et al., 1990). In general, however, Na strongly predominates over K, Cs and Ca in low cordierites.

In summary, almost all natural cordierites deviate from the ideal composition. A more complete crystal chemical formula has been recently given by Geiger et al. (2000a), modified from Schreyer (1985), as

$$^{Ch}(Na,K)_{0-1}\,^{VI}(Mg,Fe^{2+},Mn,Li)_2\,^{IV}(Si,Al,Be,Fe^{2+},Fe^{3+})_9O_{18}{*}x^{Ch}(H_2O,CO_2..).$$

1.2. Exchange mechanisms in cordierite

Charge deficiency in the framework structure is balanced by the incorporation of ions on the Ch0 channel site. Several substitution schemes have been proposed to explain deviation from the ideal composition, some of which are well confirmed whilst others are still under debate, particularly with regard to their relevance for natural cordierites. The following mechanisms of coupled substitution are considered to be the most important ones in published literature:

(1) $^{Ch}Na^{+}+{}^{IV}(Mg^{2+},Fe^{2+})={}^{Ch}\square+{}^{IV}Al^{3+}$,	Schreyer (1965)
(2) $^{Ch}Na^{+}+{}^{IV}Be^{2+}={}^{Ch}\square+{}^{IV}Al^{3+}$	Černý and Povondra, 1966
(3) $^{Ch}Na^{+}+{}^{VI}Li^{+}={}^{Ch}\square+{}^{VI}Mg^{2+}$	Schreyer (1985)
(4) $^{Ch}Na^{+}+{}^{IV}Al^{3+}={}^{Ch}\square+{}^{IV}Si^{4+}$	Schreyer (1965)
(5)=[(1)–(4)]: $^{IV}(Mg^{2+},Fe^{2+})+{}^{IV}Si^{4+}=2^{IV}Al^{3}$,	Schreyer (1985)
(6)=[(2)–(4)]: $^{IV}Be^{2+}+{}^{IV}Si^{4+}=2^{IV}Al^{3+}$	Schreyer (1965)
(7)=[(3)–(4)]: $^{VI}Li^{+}+{}^{IV}Si^{4+}={}^{VI}Mg^{2+}+{}^{IV}Al^{3+}$	Schreyer and Yoder (1964)

In terms of exchange vectors, (5)–(7) are linear combinations of (1)–(4).

1.3. Exchange vectors introducing Li and Be

A strong correlation of both Li and Be with Na [vectors (2) and (3)] has been well established by various authors (e.g., Gordillo et al., 1985; Černý et al., 1997) and explained by the presence of abundant Na in pegmatites and metapelites. Na can easily enter the channel and charge balance Be and Li, which have a relatively high crystal chemical affinity for the $T_1$1 and M sites in cordierite respectively. Field evidence for mechanism (7) appears contradictory: Kalt et al. (1998) found a correlation, whilst Černý et al. (1997) clearly state that this mechanism is not relevant for their cordierites. $^{Ch}Ca^{2+}+2^{IV}Be^{2+}={}^{Ch}\square+2^{IV}Al^{3+}$is a rare coupled substitution mechanism in nature, reported by Grew et al. (2000). Other Li and Be substitution vectors not involving Na or K have been investigated experimentally: according to Kirchner et al. (1984) and Schreyer (1985), $^{VI}Li^{IV}Si^{VI}Mg_{-1}{}^{IV}Al_{-1}$ (7) and $^{Ch}Li^{VI}Li^{Ch}\square_{-1}{}^{VI}Mg_{-1}$ are possible, but $^{Ch}Li^{IV}Al\ ^{Ch}\square_{-1}{}^{IV}Si_{-1}$ does not seem to be operative. $^{IV}Be^{IV}Si^{IV}Al_{-2}$ (6) was found to operate in experimental systems, not only in Na-free environments (Hölscher et al., 1986), but also in metapelitic compositions at high temperatures, i.e., above the solidus (Evensen and London, 2003).

1.4. Other exchange vectors

Since natural cordierites usually have (Na+K)> (Li+Be), another mechanism must cause additional Na or K to enter the structure. Schreyer (1985) lists three potential candidates: $^{Ch}Na^{IV}\,Al^{Ch}\square_{-1}{}^{IV}Si_{-1}$ (4), $^{Ch}Na^{IV}\,Mg^{Ch}\square_{-1}{}^{IV}Al_{-1}$ (1) and $^{Ch}Na_2^{IV}Mg_{-1}$ and then points out that experiments have confirmed a limited extent of solid solution via mechanism (4). Wolfsdorff and Schreyer (1992) experimentally investigated four substitution schemes for cordierite in the system NMAS: $^{Ch}Na+{}^{IV}Al={}^{Ch}\square+{}^{IV}Si$ (4), $^{Ch}Na+{}^{IV}Si={}^{VI}Mg+{}^{IV}Al$, $^{Ch}Na+{}^{IV}Mg={}^{Ch}\square+{}^{IV}Al$ (1) and $^{Ch}Na+{}^{VI}Na={}^{Ch}\square+{}^{VI}Mg$. They found a considerable range of miscibility on all for pseudobinary joins (50%, 20%, 25% and 10%, respectively). Mottana et al. (1983) invoked Na_2Mg_{-1} as mechanism $^{Ch}Na_2^{VI}\square{}^{Ch}\square_{-2}Mg_{-1}$ for a natural cordierite. The presence of Mg or Fe^{2+}in tetrahedral coordination on the $T_1$1-site was confirmed by structural and spectroscopic investigations of natural cordierites (Vance and Price, 1984; Geiger et al., 2000a; Malcherek et al., 2001). According to Geiger et al. (2000a), Fe^{2+}enters

the $T_1$1-site by exchange mechanism (1), i.e., $^{Ch}Na+^{IV}Fe=^{Ch}\square+^{IV}Al$. Kalt et al. (1998) and Malcherek et al. (2001) mention mechanism (1) as possibly relevant for their cordierites.

Solid solutions along the $^{IV}(Mg^{2+},Fe^{2+})+^{IV}Si^{4+}=$ $^{IV}2Al^{3+}$exchange (5) have been synthesized experimentally by several workers (Iiyima, 1955; Schreyer and Schairer, 1961; Smart and Glasser, 1977), but their significance for natural cordierites has yet to be confirmed. It should be noted that the reverse vector $2AlMg_{-1}Si_{-1}$, starting from the ideal cordierite composition, is not equivalent structurally, because 1 Al would be incorporated on an octahedral site: $^{VI}Al+^{IV}Al=^{VI}Mg+^{IV}Si$. To our knowledge, Al enrichment by this reverse vector (5) has not yet been observed (however, see discussion of our sample TUB-1 below).

Whilst substitution mechanisms (2) and (3) clearly operate in natural cordierites, the role of the other coupled substitution mechanisms remains unclear, mostly due to Li and Be not being analysed and/or a lack of sufficient analytical accuracy.

1.5. Material

Available information about the locality, rock type, metamorphic facies, mineral assemblage and *P–T* conditions of the investigated cordierites are summarized in Appendix B. Contamination due to traces of mineral intergrowth or fluid inclusions was avoided by careful mineral separation under the microscope. Between 20 and 120 mg of pure, gem-quality cordierite were hand-picked for H_2O and CO_2 determination, and about 40–60 mg for investigation by ICP-MS. Samples for coulrimetric titration and ICP-MS were ground in an agate mortar under isopropanol to avoid oxidation of ferrous to ferric iron, and dried at 110 °C for 8 h.

Several grains from each sample were embedded in epoxy holders and checked by BSE imaging for chemical homogeneity. In most cases, two or more grains from each sample were analysed by electron microprobe; chemical homogeneity was confirmed in each case (see values for standard deviation in Table 1). Most of the investigated samples have also been used previously and various properties characterized by other workers (see Appendix B).

2. Methods

2.1. Coulometric titration for H_2O and CO_2

Karl–Fischer titration: the water content of the cordierites was determined after thermal dehydration (1300 °C) using Karl–Fischer titration (KFT). A description of the apparatus used in this study and of the analytical procedures is given by Behrens and Stuke (submitted for publication). In crushed crystalline, material transport distances are short and H_2O can migrate rapidly out of the sample via fractures and open pores. Hence, water can be extracted completely down to several hundreds of ppm H_2O. The reliability of the method was checked by analysing materials with a known water content (rock standards; hydrous minerals such as muscovite, biotite, phlogopite or chlorite; staurolite; glasses synthesized with a well-defined amount of H_2O (see Behrens et al., 1996; Koch-Müller et al., 1997). Based on these analyses the maximum uncertainty in the titration rate is estimated to be ± 0.02 μg/s. However, duplicate analyses of cordierites show that the reproducibility of the measurements can be better than the above estimate.

CO_2 determination: The carbon content of the crystals was measured after thermal extraction (1200 °C) using CO_2 coulometric titration (Deltromat 500, Deltronik). A detailed description of the analytical technique is given in Behrens et al. (submitted for publication). Since CO_2 coulorimetric titration is an absolute method, no standards are required for calibration. The reliability of the method was tested using carbon-bearing rock powders that had been analysed in two other laboratories. The agreement between the measurements was better than 5% relative for materials containing 0.5 and 1.6 wt.% carbon (Behrens et al., submitted for publication).

2.2. Electron microprobe analysis (EMPA)

Chemical analyses were obtained with a Jeol electron microprobe (JXA-8900R) at operating conditions of 15 keV and 20 nA. The standards were either from the Smithsonian Institution's National Museum of Natural History (Jarosewich et al., 1980) or commercial MAC standards (Micro-Analysis Consultants, UK)—SiK_α: wollastonite (MAC), AlK_α: syn corundum (USNM657S), FeK_α: fayalite (USNM

Table 1
Chemical analyses of natural cordierites

Sample	TA-2	88593	2630	84-265-1	C004	G155a	TUB-1	106886	TA-4	CL-97-2	VS-1	VS-2	VS-3	42/IA	T393	40-6	25GecoMine	TA5
n[a]	127/5	130/7	63/2	26/1	32/2	30/2	95/5	26/2	52/2	50/2	70/2	23/1	200/2	30/2	22/1	199/8	86/6	49/2
SiO_2	48.49 (15)[b]	48.49 (13)	48.36 (15)	49.04 (10)	49.68 (16)	49.62 (17)	45.79 (15)	49.47 (13)	49.33 (14)	49.53 (15)	48.75 (12)	48.94 (15)	48.63 (15)	49.65 (12)	48.68 (13)	49.34 (13)	49.02 (15)	49.28 (22)
Al_2O_3	31.21 (12)	31.20 (13)	30.94 (15)	32.89 (13)	33.13 (15)	33.30 (13)	31.93 (13)	33.01 (12)	33.19 (13)	33.33 (13)	32.93 (11)	33.13 (13)	32.80 (11)	33.17 (16)	32.88 (19)	33.10 (12)	33.10 (13)	33.13 (14)
FeO[c]	6.21 (15)	6.79 (12)	6.24 (12)	5.28 (08)	2.29 (08)	2.62 (07)	16.22 (20)	1.27 (05)	3.05 (09)	4.38 (10)	6.41 (11)	6.21 (10)	5.60 (11)	2.34 (08)	7.04 (14)	3.68 (09)	4.60 (11)	4.26 (11)
MgO	8.74 (12)	8.59 (07)	8.72 (08)	10.12 (06)	12.09 (13)	12.40 (09)	2.18 (03)	12.86 (08)	11.77 (08)	10.83 (08)	9.44 (09)	9.60 (09)	10.04 (07)	12.54 (09)	9.03 (09)	11.51 (09)	10.53 (09)	10.97 (12)
MnO	0.36 (04)	0.38 (04)	0.43 (03)	0.23 (02)	0.05 (02)	0.04 (01)	0.70 (04)	tr.	0.07 (01)	0.05 (01)	0.07 (02)	0.12 (02)	0.05 (02)	0.03 (01)	0.12 (02)	0.05 (02)	0.22 (02)	0.09 (03)
ZnO[d]	*tr.*[e]	*0.02*	*n.a.*	*0.01*	*tr.*	*tr.*	*tr.*	*tr.*	*tr.*	*n.a.*	*0.02*	*0.02*	*0.02*	*tr.*	*tr.*	*tr.*	*0.07*	*0.10*
CaO	b.d.l.[f]	b.d.l.	b.d.l.	b.d.l.	0.03 (01)	b.d.l.	0.04 (01)	b.d.l.	b.d.l.	b.d.l.	b.d.l.	b.d.l.	b.d.l.	b.d.l.	b.d.l.	b.d.l.	b.d.l.	b.d.l.
BeO[d]	**0.893**	*0.832*	*n.a*	0.006	*0.061*	*0.007*	*0.005*	*0.008*	*0.002*	*n.a.*	*0.005*	*0.008*	*0.004*	*0.008*	*0.038*	*0.020*	*0.002*	*0.039*
Li_2O[d]	**0.188**	*0.155*	*n.a*	0.072	*0.060*	*0.014*	*0.110*	*0.001*	*0.006*	*n.a*	*0.013*	*0.004*	*0.000*	*0.001*	*0.001*	*0.005*	*0.040*	*0.008*
K_2O	b.d.l.	b.d.l.	b.d.l.	b.d.l.	b.d.l.	b.d.l.	b.d.l.	b.d.l.	b.d.l.	b.d.l.	b.d.l.	b.d.l.	0.02(01)	b.d.l.	b.d.l.	b.d.l.	b.d.l.	b.d.l.
Na_2O	1.40 (09)	1.36 (03)	1.40 (06)	0.41 (02)	0.51 (04)	0.43 (01)	0.55 (03)	0.32 (03)	0.21 (02)	0.08 (01)	0.11 (01)	0.06 (01)	0.10 (01)	0.33 (02)	0.07 (01)	0.28 (02)	0.28 (02)	0.25 (04)
H_2O	n.a.[g]	2.25 (02/1)[h]	2.34 (02/1)	1.28 (01/2)	1.47 (02/6)	1.46 (07/3)	1.67 (02/5)	n.a.	0.97 (05/1)	0.53 (02/1)	0.75 (02/1)	n.a.	0.36 (02/1)	1.21 (08/2)	n.a.	1.04 (01/1)	1.29 (02/1)	2.06 (08/3)
CO_2	n.a.	n.a.	n.a.	0.54 (02/1)	0.66 (03/2)	0.20 (02/3)	0.14 (02/2)	n.a.	1.47 (03/1)	1.36 (02/2)	1.32 (02/3)	n.a.	1.97 (02/4)	0.59 (02/2)	n.a.	0.77 (01/1)	1.25 (02/1)	0.20 (01/2)
Total	97.48 (35)	100.06 (29)	98.44 (30)	99.87 (26)	100.03 (37)	100.08 (33)	99.32 (36)	96.94 (23)	100.06 (24)	100.06 (28)	99.82 (25)	98.09 (29)	99.59 (27)	99.85 (26)	97.82 (37)	99.87 (26)	100.40	100.30
Li (ppm)	**873**[i]	*720*[j]	n.a.	**247**/*332*	279	**62**/*63.0*	*509*	**6.2**	*27.6*	n.a	*60.7*	**10.0**/*20.8*	*0*	*5.57*	*5.83*	*21.3*	*186*	**11**/*36.9*
Be (ppm)	**3217**	*2996*	n.a.	**21**/*21.2*	218	**40**/*24.0*	*17.1*	**30**	*8.87*	n.a.	*19.5*	**39**/*29.5*	*15.6*	*27.5*	*136*	*71.2*	*6.68*	**140**/*140*
B (ppm)	**1.12**	n.a	n.a.	**3.9**	n.a	**1.3**	n.a	**3.3**	n.a	n.a	n.a	**0.56**	n.a.	n.a.	n.a.	n.a.	n.a.	**0.80**
F (ppm)	**14**	n.a	n.a.	**11**	n.a.	**12**	n.a.	**12**	n.a.	n.a.	n.a.	**8**	n.a.	n.a.	n.a.	n.a.	n.a.	**16**
Si	5.000 (11)	5.000 (10)	5.080 (11)	5.002 (08)	5.004 (10)	4.991 (11)	4.958 (07)	5.007 (11)	4.996 (11)	5.013 (11)	5.003 (07)	5.001 (07)	5.000 (10)	4.999 (11)	5.004 (10)	4.995 (10)	4.994 (10)	4.997 (10)
Al	3.793 (13)	3.791 (10)	3.831 (15)	3.953 (10)	3.933 (13)	3.932 (11)	4.075 (11)	3.937 (11)	3.962 (13)	3.972 (11)	3.984 (10)	3.990 (10)	3.974 (11)	3.935 (14)	3.984 (11)	3.949 (11)	3.974 (11)	3.958 (12)
Be	0.221	0.206	n.a.	0.001	0.015	0.002	0.001	0.002	0.001	n.a.	0.001	0.002	0.001	0.002	0.009	0.005	0.000	0.009
[IV]	9.014 (11)	8.997 (08)	8.911 (11)	8.956 (07)	8.952 (11)	8.925 (08)	9.034 (11)	8.946 (07)	8.959 (08)	8.984 (05)	8.989 (12)	8.993 (12)	8.975 (08)	8.936 (09)	8.997 (08)	8.949 (08)	8.968 (09)	8.964 (13)
Fe	0.536 (13)	0.585 (10)	0.548 (11)	0.451 (07)	0.193 (07)	0.219 (06)	1.469 (16)	0.107 (05)	0.259 (07)	0.370 (09)	0.550 (10)	0.531 (10)	0.482 (11)	0.197 (07)	0.605 (13)	0.311 (08)	0.392 (10)	0.361 (10)
Mg	1.343 (17)	1.320 (10)	1.366 (12)	1.539 (09)	1.816 (16)	1.851 (11)	0.351 (6)	1.940 (11)	1.777 (11)	1.634 (12)	1.445 (14)	1.463 (14)	1.540 (12)	1.866 (12)	1.384 (11)	1.736 (13)	1.599 (13)	1.658 (17)
Mn	0.031 (04)	0.034 (04)	0.038 (03)	0.020 (02)	0.004 (03)	0.003 (2)	0.064 (03)	tr.	0.006 (02)	0.005 (02)	0.006 (02)	0.010 (02)	0.004 (02)	0.003 (01)	0.011 (02)	0.004 (02)	0.019 (02)	0.008 (03)
Zn	tr.	0.001	n.a.	0.001	tr.	tr.	tr.	tr.	tr.	n.a.	0.001	0.001	0.002	tr.	tr.	tr.	0.005	0.008
Li	0.078	0.064	n.a.	0.029	0.024	0.005	0.048	0.001	0.002	n.a.	0.005	0.002	0.000	0.000	0.001	0.002	0.016	0.003
[VI]	1.988 (22)	2.004 (16)	1.951 (17)	2.039 (12)	2.037 (18)	2.079 (14)	1.932 (18)	2.048 (13)	2.044 (14)	2.009 (10)	2.008 (19)	2.007 (19)	2.027 (15)	2.066 (15)	2.001 (14)	2.054 (14)	2.026 (15)	2.037 (21)
Na	0.280 (19)	0.271 (08)	0.286 (13)	0.081 (04)	0.099 (09)	0.083 (04)	0.115 (04)	0.064 (06)	0.041 (04)	0.016 (03)	0.023 (03)	0.011 (03)	0.020 (02)	0.064 (05)	0.013 (02)	0.056 (04)	0.056 (04)	0.050 (09)
K	b.d.l.	b.d.l.	b.d.l.	b.d.l.	b.d.l.	b.d.l.	b.d.l.	b.d.l.	b.d.l.	b.d.l.	b.d.l.	b.d.l.	0.002 (01)	b.d.l.	b.d.l.	b.d.l.	b.d.l.	b.d.l.
Ca	b.d.l.	b.d.l.	b.d.l.	b.d.l.	0.003 (01)	b.d.l.	0.004 (01)	b.d.l.	b.d.l.	b.d.l.	b.d.l.	b.d.l.	b.d.l.	b.d.l.	b.d.l.	b.d.l.	b.d.l.	b.d.l.
[ch]	0.280 (19)	0.271 (08)	0.286 (13)	0.081 (04)	0.102 (10)	0.083 (04)	0.119 (05)	0.064 (06)	0.041 (04)	0.016 (03)	0.023 (03)	0.011 (03)	0.022 (02)	0.064 (05)	0.013 (02)	0.056 (04)	0.056 (04)	0.050 (09)
X_{Fe}[k]	0.269 (19)	0.292 (08)	0.281 (13)	0.221 (03)	0.096 (03)	0.106 (02)	0.760 (03)	0.052 (02)	0.127 (03)	0.184 (04)	0.274 (04)	0.265 (04)	0.238 (05)	0.095 (03)	0.304 (5)	0.152 (04)	0.193 (04)	0.177 (04)

Sample	TA-1	126178F	C005	WYO-2	118871	HO6	CTsiM	C006	129875	7114	7107	TA-6	TA3	C2623	DA-1	CMikM
n	98/3	25/2	31/2	83/4	41/2	63/5	75/3	33/1	30/1	91/5	30/3	25/2	33/2	29/2	60/2	26/2
SiO_2	50.03 (12)	48.28 (16)	49.61 (17)	49.68 (15)	49.10 (13)	47.71 (16)	49.67 (15)	49.62 (12)	49.76 (16)	48.67 (12)	48.88 (12)	49.83 (17)	49.46 (10)	49.34 (15)	49.76 (14)	49.26 (16)
Al_2O_3	33.71 (15)	32.61 (14)	33.49 (10)	33.35 (15)	33.01 (12)	32.15 (13)	33.31 (13)	33.32 (18)	33.60 (13)	32.83 (10)	32.94 (10)	33.37 (17)	33.13 (13)	33.05 (14)	33.26 (15)	33.22 (13)
FeO	1.07 (06)	8.93 (16)	4.55 (09)	2.53 (08)	3.73 (09)	12.20 (14)	2.57 (07)	2.63 (07)	1.06 (06)	6.58 (11)	5.84 (10)	1.51 (05)	2.37 (07)	2.32 (07)	2.11 (08)	4.95 (10)
MgO	12.90 (07)	7.92 (08)	10.75 (07)	12.19 (09)	11.13 (07)	5.47 (05)	12.15 (07)	11.99 (08)	12.99 (07)	9.44 (06)	9.86 (08)	13.04 (08)	12.28 (08)	12.34 (9)	12.56 (07)	10.57 (09)
MnO	0.07 (03)	0.18 (02)	0.06 (01)	0.05 (01)	0.34 (01)	0.67 (03)	0.02 (01)	tr.	tr.	0.04 (02)	0.04 (02)	tr.	0.067	0.07 (02)	0.03 (01)	0.12 (02)
ZnO	*tr.*	*n.a.*	*tr.*	*tr.*	*n.a.*	*0.01*	tr.	tr.	tr.	n.a.	n.a.	tr.	n.a.	tr.	n.a.	n.a.
CaO	b.d.l.	b.d.l.	b.d.l.	b.d.l.	b.d.l.	b.d.l.	b.d.l.	b.d.l.	b.d.l.	b.d.l.	b.d.l.	b.d.l.	0.02 (01)	b.d.l.	b.d.l.	0.02 (1)
BeO	*0.008*	**0.003**	*0.018*	0.004	**0.002**	*0.118*	*0.000*	*0.001*	*0.010*	n.a.	n.a.	*0.004*	n.a.	*0.005*	n.a.	n.a.
Li_2O	*0.029*	**0.006**	*0.017*	0.012	**0.036**	*0.023*	*0.006*	*0.007*	*0.005*	n.a.	n.a.	*0.006*	n.a.	*0.015*	n.a.	n.a.
K_2O	b.d.l.	b.d.l.	b.d.l.	b.d.l.	b.d.l.	0.14 (01)	0.02 (01)	b.d.l.	0.04 (01)	b.d.l.	b.d.l.	b.d.l.	b.d.l.	b.d.l.	b.d.l.	b.d.l.
Na_2O	0.23 (02)	0.10 (02)	0.13 (01)	0.30 (06)	0.38 (02)	0.20 (02)	0.02 (1)	0.18 (01)	0.15 (02)	0.09 (02)	0.10 (01)	0.37 (01)	0.36 (02)	0.41 (02)	0.35 (02)	0.06(01)
H_2O	1.33 (02/1)	n.a.[f]	0.89 (07/2)	1.21 (02/2)	n.a.	0.37 (01/1)	1.15 (03/5)	1.12 (01/7)	0.38 (01/6)	0.26 (01/1)	0.80 (0/12)	n.a.	1.44 (02)	1.33 (07/3)	1.19 (01)	0.33 (02/2)
CO_2	0.53 (02/2)	n.a.	0.12 (02/2)	0.51 (01/2)	n.a.	0.28 (02/2)	0.90 (02/3)	1.02 (02/2)	1.74 (03/3)	1.23 (02/1)	1.44 (01/1)	n.a.	n.a	1.20 (01/2)	0.75 (02)	0.88 (01)
Total	99.89 (26)	98.03 (40)	99.63 (21)	99.82 (30)	97.73 (23)	99.35 (33)	100.01 (27)	99.89 (27)	99.73 (32)	99.14 (18)	99.89 (27)	98.22 (34)	99.10 (28)	100.05 (28)	100.02 (28)	99.41 (26)
Li (ppm)	*136*	**27.3**	*78.0*	*56.8*	**168**	*107*	*28.9*	*32.3*	*24.9*	n.a.	n.a.	*26.0*	n.a.	*69.1*	n.a.	n.a.
Be (ppm)	*29.7*	**10.1**	*63.9*	*12.6*	**7.8**	*425*	*1.19*	*4.77*	*34.5*	n.a.	n.a.	*15.1*	n.a.	*16.6*	n.a.	n.a.
B (ppm)	n.a.	**0.65**	n.a.	n.a.	**3.8**	n.a.	n.a.	n.a.	n.a.	n.a.	n.a.	n.a.	n.a.	n.a.	n.a.	n.a.
F (ppm)	n.a.	**6**	n.a.	n.a.	**10**	n.a.	n.a.	n.a.	n.a.	n.a.	n.a.	n.a.	n.a.	n.a.	n.a.	n.a.
Si	5.000 (10)	5.002 (13)	5.003 (09)	4.997 (11)	4.993 (10)	4.998 (08)	5.002 (10)	5.006 (12)	4.993 (10)	5.004 (08)	5.008 (08)	4.995 (11)	4.996 (09)	4.992 (11)	4.999 (10)	5.000 (12)
Al	3.970 (12)	3.982 (11)	3.980 (12)	3.953 (12)	3.956 (11)	3.954 (10)	3.954 (13)	3.962 (13)	3.974 (11)	3.978 (11)	3.978 (08)	3.935 (12)	3.944 (10)	3.940 (11)	3.938 (11)	3.975 (11)
Be	0.002	0.001	0.004	0.001	0.001	0.030	0.000	0.000	0.002	n.a.	n.a.	0.001	n.a.	0.000	n.a.	n.a.
[IV]	8.971 (07)	8.984 (09)	8.987 (09)	8.951 (11)	8.950 (08)	8.998 (07)	8.956 (06)	8.969 (06)	8.970 (06)	8.982 (07)	8.985 (08)	8.930 (06)	8.940 (07)	8.933 (07)	-148.937 (06)	8.975 (09)
Fe	0.089 (06)	0.773 (13)	0.384 (08)	0.213 (07)	0.317 (08)	1.069 (11)	0.216 (06)	0.222 (06)	0.089 (05)	0.565 (10)	0.500 (09)	0.126 (04)	0.200 (06)	0.196 (06)	0.177 (07)	0.420 (08)
Mg	1.921 (10)	1.223 (10)	1.616 (09)	1.827 (14)	1.688 (10)	0.854 (08)	1.825 (10)	1.803 (10)	1.943 (08)	1.447 (10)	1.505 (11)	1.944 (09)	1.848 (10)	1.861 (11)	1.881 (10)	1.599 (13)
Mn	0.006 (03)	0.016 (02)	0.005 (02)	0.004 (02)	0.029 (02)	0.059 (03)	0.001 (01)	tr.	tr.	0.003 (02)	0.003 (02)	tr.	0.006 (02)	0.006 (02)	0.003 (01)	0.011 (01)
Zn	tr.	n.a.	tr.	tr.	n.a.	0.001.	tr.	tr.	tr.	n.a.	n.a.	tr.	n.a.	tr.	n.a.	n.a.
Li	0.012	0.002	0.007	0.005	0.015	0.010	0.003	0.003	0.002	n.a.	n.a.	0.002	n.a.	0.006	n.a.	n.a.
[VI]	2.028 (12)	2.014 (17)	2.011 (14)	2.049 (17)	2.049 (14)	1.993 (13)	2.045 (10)	2.028 (11)	2.034 (10)	2.016 (11)	2.008 (14)	2.073 (11)	2.055 (11)	2.069 (14)	2.061 (11)	2.030 (16)
Na	0.044 (04)	0.019 (04)	0.025 (04)	0.058 (12)	0.076 (04)	0.041 (04)	0.040 (03)	0.034 (03)	0.029 (03)	0.019 (04)	0.020 (02)	0.072 (03)	0.070 (04)	0.080 (04)	0.068 (04)	0.011 (03)
K	b.d.l.	b.d.l.	b.d.l.	b.d.l.	b.d.l.	0.019 (02)	0.003 (01)	b.d.l.	0.05 (1)	b.d.l.	b.d.l.	b.d.l.	b.d.l.	b.d.l.	b.d.l.	b.d.l.
Ca	b.d.l.	b.d.l.	b.d.l.	b.d.l.	b.d.l.	b.d.l.	b.d.l.	b.d.l.	b.d.l.	b.d.l.	b.d.l.	b.d.l.	0.002 (01)	b.d.l.	b.d.l.	0.002 (01)
[ch]	0.044	0.019 (04)	0.025 (04)	0.058 (04)	0.076 (04)	0.060 (05)	0.042 (03)	0.034 (03)	0.034 (03)	0.019	0.020	0.072	0.072 (04)	0.080 (04)	-140.068	0.013 (04)
X_{Fe}	0.044 (03)	0.384 (04)	0.191 (03)	0.104 (03)	0.155 (03)	0.536 (04)	0.106 (03)	0.109 (03)	0.044 (03)	0.280 (04)	0.249 (04)	0.061 (02)	0.098 (03)	0.095 (02)	0.086 (03)	0.207 (03)

If both SIMS and ICP-MS data are available, the latter had been used for the calculation of the chemical formula. The chemical formulae of cordierites were calculated on the basis of 36 positive charges.

[a] Number of analyses/grains.

[b] Numbers in brackets are 1σ standard deviations in terms of the last two digits.

[c] All Fe as FeO.

[d] ppm converted into wt.%.

[e] tr.=trace amounts.

[f] b.d.l=below detection limit.

[g] n.a.=not analysed.

[h] (02/1)=error propagation/number of titrations.

[i] Bold numbers=values obtained by SIMS.

[j] Italic numbers=values obtained by ICP-MS.

[k] X_{Fe}=Fe/(Fe+Mg+Mn+Zn).

85276), MgK_α: forsterite (MAC), MnK_α: spessartine (MAC), NaK_α: anorthoclase (USNM 133868), KK_α: microcline (USNM 143966), CaK_α: wollastonite (MAC), TiK_α: benitoite (USNM 86539). Raw counts were corrected with a CITZAF- procedure. The chemical formula of cordierites were calculated on the basis of 36 positive charges.

2.3. Secondary ion mass spectrometry analyses (SIMS)

A Cameca IMS-4f ion microprobe was used for the analyses of Li, Be, B and F at the CNR Centro di Studio per la Cristallochimica e Cristallographia in Pavia, under analytical conditions described in full by Ottolini et al. (1993). The accuracy for Li, Be, B and F was typically better than 10% relative.

2.4. Inductively coupled plasma mass spectrometry (ICP-MS)

Trace element concentrations were determined from pressurised mixed acid HF–HNO_3–HCl–$HClO_4$ digests dissolved in 2% (v/v) HNO_3 (Garbe-Schönberg, 1993). Sample weights were 40–60 mg. The following 43 elements were measured with an Agilent 7500c quadrupole-based ICP-MS under standard operating conditions using the isotopes: Li-7, Be-9, V-51, Cr-52, Mn-55, Co-59, Ni-60, Cu-63, Zn-66, Ga-71, Rb-85, Sr-88, Y-89, Zr-90, Nb-93, Mo-98, Ag-109, Cd-114, Sn-120, Sb-121, Cs-133, Ba-138, La-139, Ce-140, Pr-141, Nd-146, Sm-147, Eu-151, Gd-157, Tb-159, Dy-163, Ho-165, Er-166, Tm-169, Yb-172, Lu-175, Hf-178, Ta-181, W-182, Tl-205, Pb-206-208, Th-232, and U-238. A freely aspirating PFA micronebuliser was used for sample uptake. In and Re (5 μg/ml) were used for internal standardisation. Results are averages from three analytical runs. For Eu and Gd, corrections were applied for O and OH interferences, respectively. Precision, as estimated from replicate digests and replicate measurements, was <3% relative for most elements with concentrations over 0.5 ppm, and <10% relative for Be and Cr. Accuracy was controlled by international rock/mineral reference standards feldspar JF-1, K-feldspar FK-N, albite Al-1, phlogopite IWG Mica-Mg.

3. Results

The results of the EMPA analyses, the coulometric titration for H_2O (KFT) and CO_2, and the SIMS and ICPMS analyses are listed in Table 1. Where both SIMS and ICPMS data were available for Li and Be, the latter was used for the calculation of cordierite formula. For some samples, H_2O and CO_2 and/or trace elements could not be determined because the amount of material was too small, or cordierite was too finely intergrown with other phases for a clean separation.

The Si cations p.f.u. are close to 5.00 (±0.01) and the Al cations p.f.u. are significantly below 4.00 for most samples. Following a standard formula recalculation procedure, most of the investigated cordierites have “excess occupation” of the octahedral position. In most of the investigated cordierites the alkali and alkaline earth metals, except for sodium and magnesium, are trace elements (below 0.10 wt.%). The only exceptions are samples TA-2, 88593, TUB-1 and HO6, where Li_2O, BeO and K_2O contents are above 0.1 wt.%. K_2O and CaO are below the limit of detection (0.02 wt.%) of the electron microprobe for most of these cordierites. TiO_2 is below the detection limit of 0.06 wt.% of the electron microprobe. Mn values obtained by ICPMS lie within the standard deviation of EMPA-values for most of the cordierites, with the only notable exceptions being the Fe-rich cordierites TUB-1 and HO6.

The cordierites investigated contain up to 873 ppm Li and 3217 ppm Be. B and F contents are generally low: 0.52–3.9 and 8–16 ppm, respectively.

The concentration of the large ion lithophile elements $Pb^{2+}$and Tl^{+}, the second series transition metals Y^{3+}, $Ag^{1+}$and Cd^{2+}, the high field-strength elements Hf^{4+}, Nb^{5+}, Ta^{5+}, U^{4+}, Mo^{6+}, Sn^{4+}, W^{6+}, the rare earth elements, and the actinides Th^{4+} and U^{4+} as well as $Sb^{2+}$are always lower than 10 ppm and very commonly lower than 1 ppm. The large ion lithophile elements content ranges between 0.430 and 21.7 ppm for Rb^{+}, between 0.446 and 11.5 ppm for Sr^{2+}, between 0.112 and 41 ppm for Cs^{+} and between 1.27 and 901 ppm for Ba^{2+}. The concentration of the first series transition metals Sc^{3+}, Ti^{4+}, V^{5+}, Cr^{3+}, Co^{2+}, Ni^{2+}, Cu^{2+}, Zn^{2+} and of the second series transition metal Zr^{4+} ranges between 0.16 and 811ppm. Ga^{3+}contributes between 14.5 and 70.4 ppm.

If the trace element contents are converted into wt.% of their oxides and added together they contribute between 0.005 and 0.119 wt.% to the total and thus only affect it within its standard deviation. Together with H_2O and CO_2, as determined by the coulometric titration, the full totals range between 99.50 and 100.50 (except for TUB-1, HO6 and CMikM). These good totals, the small standard deviations of analyses and the excellent cation numbers, particularly for cordierites where Li and Be were determined, indicate a high accuracy and precision for the analyses (Table 1).

3.1. Correlations

As a first step, we have combined our own analyses with all those from published literature in which both Li and Be had been analysed (Miyashiro, 1957; Ginzburg and Stavrov, 1961; Newton, 1966; Černý and Povondra, 1966; Povondra and Čech, 1978; Schreyer et al., 1979; Armbruster and Irouschek, 1983; Povondra et al., 1984; Gordillo et al., 1985; Kalt et al., 1998, 1999; Grew et al., 1987, 1990, 1995; Bea et al., 1994; Visser et al., 1994; Černý et al., 1997; Istomin et al., 1997; Malcherek et al., 2001),

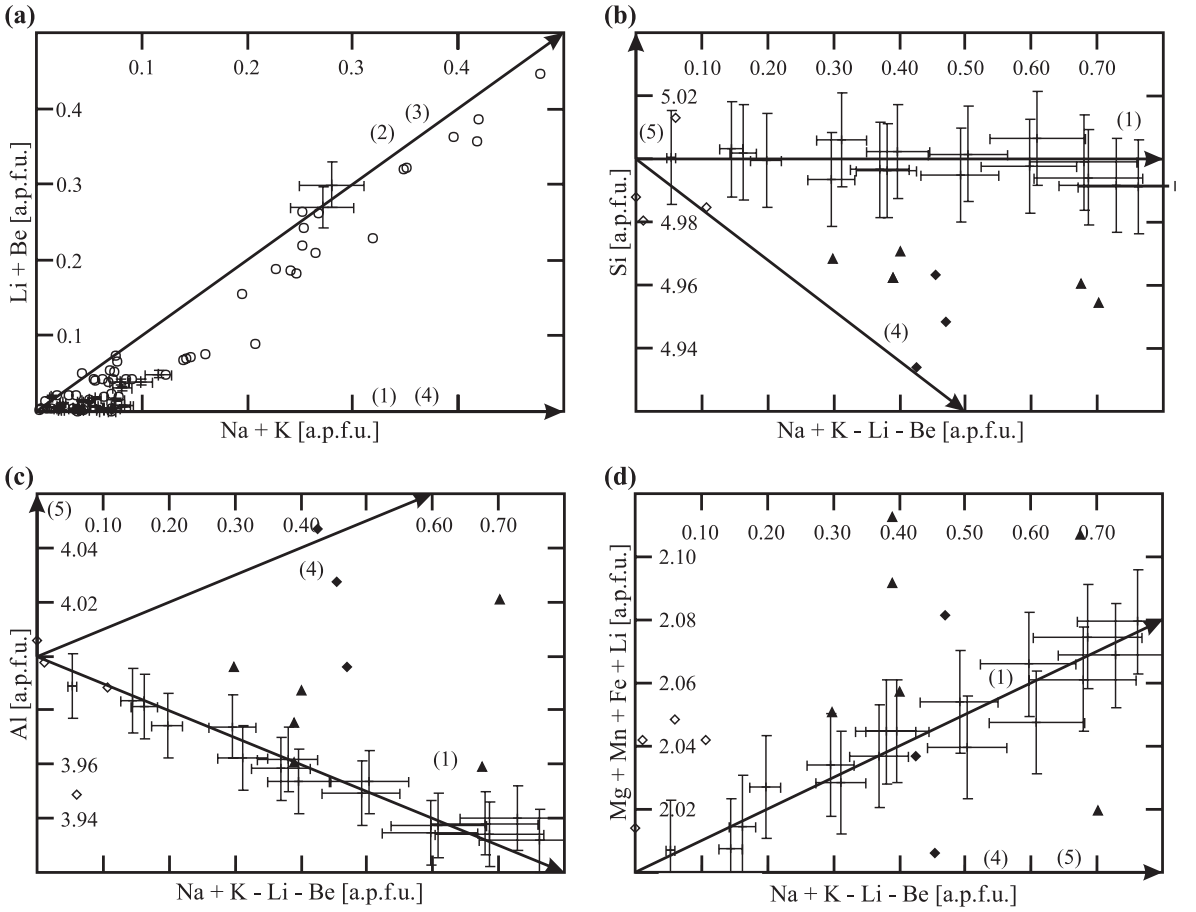

Fig. 2. (a) (Li+Be) versus (Na+K) for cordierites from the literature (circles) and our own analyses (dots with error bars, 1σ) shows a clear correlation. Most analyses plot to the right of the diagonal, indicating that additional Na is incorporated by other exchange vectors than mechanisms (2) and (3). (b)–(d) Plots of Si, Al and (Mg+Fe+Mn+Li) versus (Na+K–Li–Be), respectively, for cordierites with little or no Li and Be. Our own analyses (crosses) confirm that exchange mechanism (1) is dominant. Literature analyses (solid diamond, Armbruster and Irouschek, 1983; open diamond, Grew et al., 1990; solid triangle, Malcherek et al., 2001) have a considerable spread that cannot be explained by exchange mechanisms (4) or (5), which are shown by arrows.

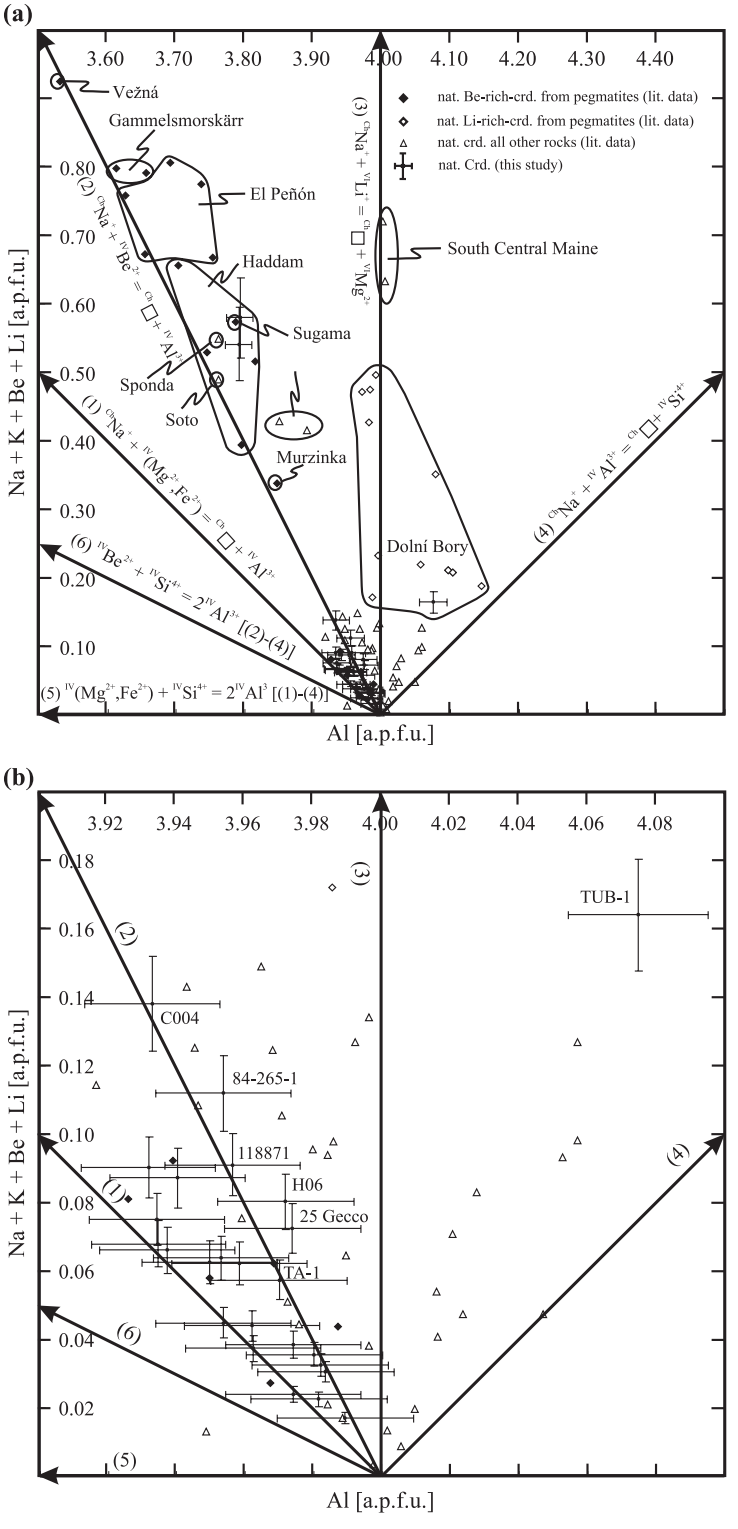
(a)
3.60
3.70
3.80
3.90
4.00
4.10
4.20
4.30
4.40
0.80
0.70
0.60
0.50
0.40
0.30
0.20
0.10
Na + K + Be + Li [a.p.f.u.]
Al [a.p.f.u.]
Vežná
Gammelsmorskärr
El Peñón
Haddam
Sugama
Sponda
Soto
Murzinka
Dolní Bory
South Central Maine
nat. Be-rich-crd. from pegmatites (lit. data)
nat. Li-rich-crd. from pegmatites (lit. data)
nat. crd. all other rocks (lit. data)
nat. Crd. (this study)
(1) $^{Ch}Na^{+} + {}^{IV}(Mg^{2+},Fe^{2+}) = {}^{Ch}\square + {}^{IV}Al^{3+}$
(2) $^{Ch}Na^{+} + {}^{IV}Be^{2+} = {}^{Ch}\square + {}^{IV}Al^{3+}$
(3) $^{Ch}Na^{+} + {}^{VI}Li^{+} = {}^{Ch}\square + {}^{VI}Mg^{2+}$
(4) $^{Ch}Na^{+} + {}^{IV}Al^{3+} = {}^{Ch}\square + {}^{IV}Si^{4+}$
(5) $^{IV}(Mg^{2+},Fe^{2+}) + {}^{IV}Si^{4+} = 2\,{}^{IV}Al^{3+}$ [(1)-(4)]
(6) $^{IV}Be^{2+} + {}^{IV}Si^{4+} = 2\,{}^{IV}Al^{3+}$ [(2)-(4)]
(b)
3.92
3.94
3.96
3.98
4.00
4.02
4.04
4.06
4.08
0.18
0.16
0.14
0.12
0.10
0.08
0.06
0.04
0.02
Na + K + Be + Li [a.p.f.u.]
Al [a.p.f.u.]
TUB-1
C004
84-265-1
118871
H06
25 Gecco
TA-1
(1)
(2)
(3)
(4)
(5)
(6)

in order to establish any significant correlations. Fig. 2a demonstrates that Li and Be correlate strongly with Na (+K), confirming the conclusion of other workers that mechanisms (2) and (3) are the dominant mechanisms for the uptake of Li and Be in natural cordierite, and most probably the only ones necessary to explain this uptake. A large quantity of analyses plot below the diagonal, indicating that an additional mechanism, e.g., mechanism (1) or (4), causes further Na uptake in cordierite. In order to discover the exchange mechanisms that operate independently of Be and Li substitution, we looked for correlations in cordierites that are virtually free of Be and Li.

Fig. 2b–d shows plots of Si, Al and (Mg+Fe+Mn+Li) versus (Na+K–Li–Be) for cordierites where Li and Be were analysed and their levels found to be near or below detection limit. These minor amounts of Li and Be found were subtracted from (Na+K) corresponding to vectors (2) and (3), so that the x-axis shows all (Na+K) remaining for other vectors as precisely as possible. In all three plots, our own data strongly indicate exchange mechanism (1) as the only other valid mechanism operating, whilst data from other authors (Armbruster and Irouschek, 1983; Grew et al., 1990; Malcherek et al., 2001) show a considerable spread.

Vectors (4) and (5) in Fig. 2b and c give the impression that they could explain the deviations, but this is clearly contradicted by Fig. 2d. A detailed inspection of each of the deviant analyses in the literature reveals that almost all of them require a somewhat different set of exchange vectors, including several new ones. These inconsistencies are, in our view, most likely due to analytical error (see Discussion).

In Fig. 3a and b, published data is combined with our results and plotted as Al (a.p.f.u.) versus Na+Be+Li (a.p.f.u.). In this diagram all seven exchange vectors (arrows) can be shown. Vector (7) coincides with (1), and is not labelled. The symbols demonstrate that most of the Be-rich or Li-rich cordierites investigated to date are from pegmatites, except for those from Alpe Sponda (Armbruster and Irouschek, 1983) and south-central Maine, USA (Ferry, 1980; Armbruster, 1986). Fig. 3a and the enlargement in Fig. 3b reveal that virtually all cordierites plot between exchange vectors (1) and (4). Most of our analyses plot in the vicinity of vectors (1) and (2). The published data scatter more broadly between mechanisms (1) and (4).

4. Discussion

The discrepancy between the smooth correlation of our analyses and the lack of correlation [except for vectors (2) and (3)] of analyses from within published literature is marked. As it was virtually impossible for us to find a reasonable consistent set of exchange vectors that would explain the majority of analyses from published literature we conclude that a larger range of analytical error (compared to our analyses) blurs the view.

Five out of 12 deviant analyses in Fig. 2b–d are from Malcherek et al. (2001), four are from Grew et al. (1990) and three are from Armbruster and Irouschek (1983). The focus of the Malcherek et al. (2001) paper is on crystallography and major elements were analysed with an energy dispersive system only, the accuracy of which is significantly less than that of a wavelength dispersive microprobe analyser. Another source of inaccuracy may be the use of an ion microprobe (SIMS) for Li and Be measurements by most groups, exceptions being ourselves and Armbruster and Irouschek (1983). From our experience, ICPMS on solutions is slightly more precise than SIMS (see Methods), and possibly also more accurate. Any incorrect Li and Be values result in incorrect Na for vectors (1) or (4) and propagate into the calculation of the remaining exchange vectors.

Only two of our own complete analyses deviate significantly from 100%: TUB-1 and HO6. Interestingly, these are the most Fe-rich cordierites. TUB-1 is from a Li-pegmatite in Dolní Bory; HO6 is from a xenolith in a volcanic rock and contains substantial K. Both deviate from the general trend of vector (1),

Fig. 3. (a) Diagram illustrating the exchange mechanisms (1)–(7) in cordierites. Chemical analyses for Be-rich cordierites (solid diamond, 21 analyses) and Li-rich cordierites (open diamond, 13 analyses) from pegmatites and from cordierites with known Be and Li content from other rock types (open triangle, 39 analyses) are taken from published literature and compared with our own results (dots with error bars, 1σ). (b) Enlarged detail of panel a. Our own analyses with significant Li and Be content are labeled for comparison with Table 1.

but the reasons (analytical error or other exchange vectors) are not clear. TUB-1 is the only analysis with Si≪5.00 and Al≫4.00. The analysis could be explained by a combination of $^{Ch}Na^{VI}Li^{Ch}\square_{-1}{}^{VI}Fe_{-1}$, $^{VI}Al^{IV}AlFe_{-1}Si_{-1}$ and $^{Ch}Na_2^{VI}\square^{Ch}\square_{-2}Fe_{-1}$, as could be the analysis by Armbruster and Irouschek (1983) of another cordierite from Dolní Bory. Other analyses of Dolní Bory cordierites (e.g., Černý et al., 1997; Malcherek et al., 2001) are not consistent enough to support a Tschermak-type exchange mechanism, but the tendency of some metamorphic cordierites as well as some from Dolní Bory to plot to the right of vector (3) in Fig. 3 indicates such a possibility. Further high-precision analyses of these and other cordierite samples from a great diversity of geological settings and *P–T* conditions are needed to establish whether other exchange vectors, in addition to vectors (1), (2) and (3), are significant for natural cordierite compositions.

4.1. Cordierites without Li and Be analyses

Most of the published cordierite analyses do not report the contents of light elements or volatiles. For any such analysis, the difference between the total wt.% measured by EMPA and 100.00 wt.% can be caused by any combination of volatiles, Li and Be, or by analytical error. Thus, the question arises whether it is possible to predict light element contents in cordierite from our knowledge of dominant exchange vectors as derived above.

Whilst volatiles have no effect on formula recalculation, unknown but significant Li and Be contents do have an effect. Consequently, we have adopted the following procedure: all analyses, both from published literature and from our own data compilation, have been recalculated, disregarding any Li and Be content (Li, Be=0), and plotted in a

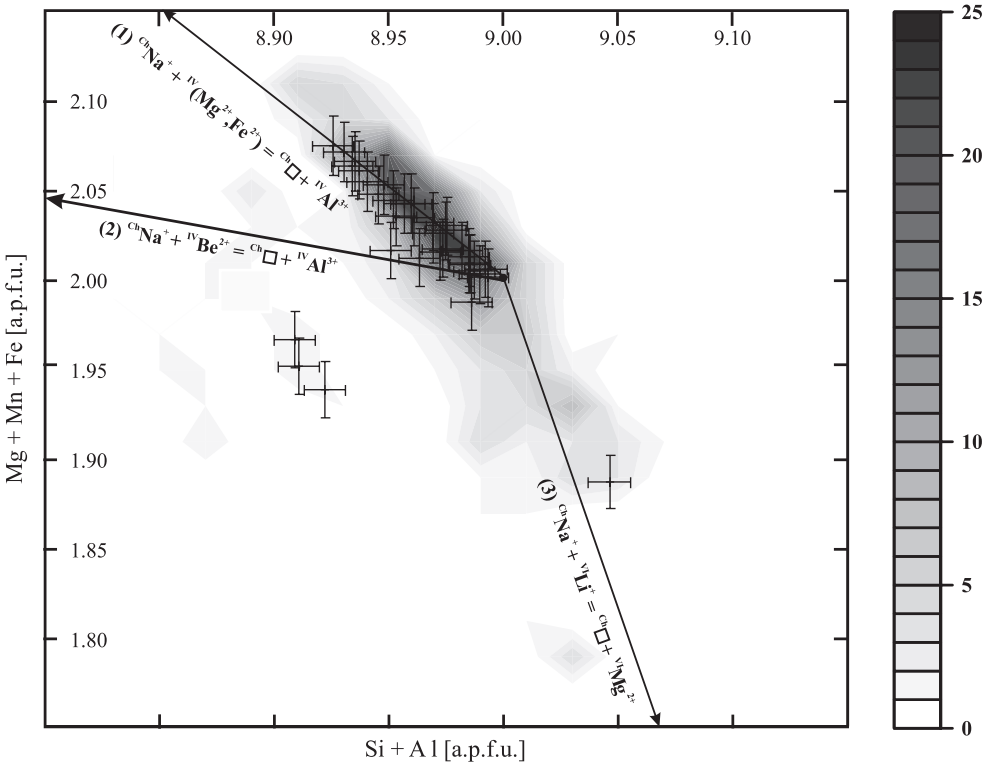

Fig. 4. Octahedral (Mg+Fe+Mn) versus tetrahedral (Si+Al) site occupancy of natural cordierites, ignoring Li and Be content (if present) for formula calculations. Comparison of our results (dots with error bars, 1σ) with data from published literature. Frequency of the published data (309 chemical analyses) is denoted by grey shading.

diagram showing octahedral (Mg+Fe+Mn) versus tetrahedral (Si+Al) site occupation (Fig. 4). Exchange vectors (1) to (3) are also shown on this diagram. The frequency of analysis points (309 analyses in total) is given by shading. Exchange vectors (2) and (3) indicate the characteristic changes in the calculated occupancy of the octahedral and tetrahedral sites obtained by neglecting an actual Be and Li content, respectively.

If exchange mechanism (1) has been operational, then (Mg+Fe)>2 and (Si+Al)<9.00 a.p.f.u, i.e., Si=5.00 and Al<4.00 a.p.f.u.

If exchange mechanism (2) has been operational but Be is not determined, then Si>5.00 a.p.f.u. and Al≪4.00. (Si+Al)<9.00 a.p.f.u. and (Mg+Fe)>2.00 a.p.f.u.

If exchange mechanism (3) has been operational but Li is not determined, then Si>5.00 a.p.f.u. and Al>4.00 a.p.f.u., (Si+Al)≫9.00 a.p.f.u. and (Mg+Fe)≪2.00 a.p.f.u.

In other words, if Be and Li are not taken into account for the formula calculations the other elements are systematically overestimated. Sample 2630 (Li and Be not analysed) plots very close to samples TA-2 and 88593 (Li and Be analysed), which are from the same locality (Haddam, see Appendix B). Si is calculated as 5.08 a.p.f.u., Al is significantly less than 4.00, and (Si+Al) less than 9.00 a.p.f.u. (Table 1), as we would expect of exchange mechanism (2). Haddam cordierites also contain Li (vector 3), thus (Mg+Fe) drops below 2.00 a.p.f.u.

If a carefully performed EMPA analysis of a cordierite plots left of the dotted lines in Fig. 5, it lies outside the range of analytical uncertainty with regard to exchange vector (1) and should be analysed for Li and/or Be. If the analysis of major elements were perfect, it would contain more than 0.02 a.p.f.u. Be and/or 0.02 a.p.f.u. Li, i.e., more than 0.086 wt.% BeO and or 0.051 wt.% Li_2O in the case of end member Mg-cordierite and more than 0.077 wt.% BeO and or 0.046 wt.% Li_2O in the case of end member Fe-cordierite (sekaninaite).

Given that mechanisms (1), (2) and (3) are the only relevant coupled substitution mechanisms, theoretical Li and Be contents can be calculated from the cordierite analysis by normalizing to 5 Si atoms p.f.u. in the idealized formula $Na_{x+y+z}{}^{VI}(Li_z\ M^{2+}_{2-z})^{IV}(Be_yM^{2+}_xAl_{4-x-y})Si_5O_{18}$ [with M^{2+}=Mg, Fe^{2+}, Mn,

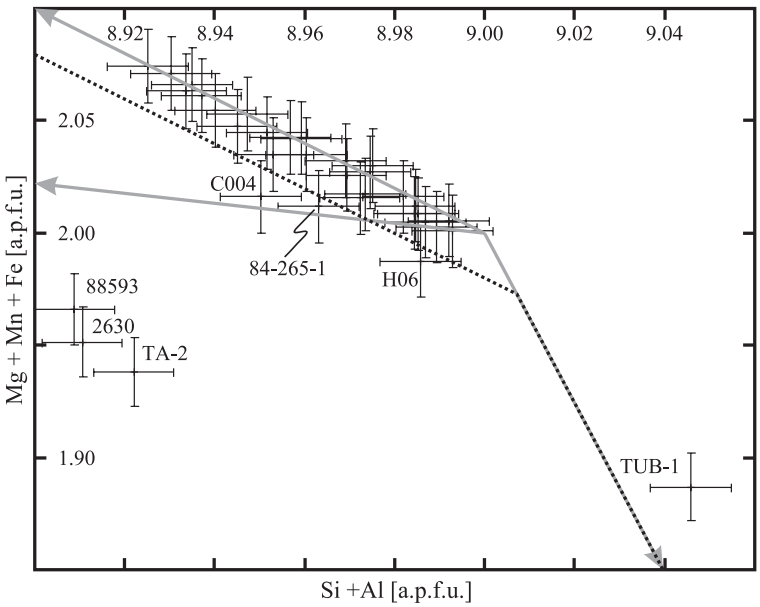

Fig. 5. Enlarged portion of Fig. 4. If an EMP analysis plots to the left of the dotted line, more than 0.02 a.p.f.u., Be and/or Li can be expected. Sample numbers of Be-rich and/or Li-rich cordierites are given.

Zn and with x, y, z corresponding to the modal amounts of vectors (1), (2) and (3), respectively].

From $Na=x+y+z$, $Al=4-y-x$, $(^{VI}M^{2+}+^{IV}M^{2+})=M^{2+}=2+x-z$, we obtain:

$$x = Al + M^{2+} + Na - 6;$$

$$y = 10 - 2Al - M^{2+} - Na;$$

$$z = Al + Na - 4.$$

The reliability of the numbers calculated is highly dependent on the accuracy of electron microprobe analyses: values below 0.02 or even 0.03 a.p.f.u. are probably not significant.

5. Conclusions

In natural cordierites, sodium is the dominant alkali metal and is incorporated mainly by the coupled substitution mechanisms (1) to (3). Substitution of Na by K^+ or Cs^+ is mostly below the detection limit. Concentrations of the first series transition elements, apart from manganese and iron, are also very low and play a negligible role in compositional variations of cordierite.

Deviation from the ideal composition in the investigated samples can be explained by the simple and linearly independent exchange vectors (1) to (3), and the homovalent substitutions of $FeMg_{-1}$, $MnMg_{-1}$ and KNa_{-1}.

The most important coupled substitution is $^{Ch}Na^+ + {}^{IV}(Mg^{2+},Fe^{2+})={}^{Ch}\square+{}^{IV}Al^{3+}$ (1) because most of the investigated cordierites show an "excess occupation" of the octahedral position and Al is significantly below 4.00 a.p.f.u.. However, the extent of this substitution seems to be limited to about 0.08 a.p.f.u. (Fig. 3b). The possibility of coupled substitution by this mechanism had been mentioned by several workers (e.g., Schreyer, 1985; Kalt et al., 1998; Malcherek et al., 2001), but its almost exclusive restriction to Be or Li poor cordierites has only become clear in the data presented above.

Beryllium is incorporated in cordierite by the coupled substitution vector (2) because analyses with Si>5.00 a.p.f.u., as would result, e.g., from exchange vector (6) $^{IV}Be^{2+}+{}^{IV}Si^{4+}=2{}^{IV}Al^{3+}$ (Schreyer, 1985) are most probably artefacts resulting either from Li and/or Be not being analysed and Si thus being overestimated, or from a general lack of analytical accuracy. Analogous arguments apply for lithium. It enters natural cordierites by mechanism (3) only. None of the cordierites analysed had (Na+K)< (Li+Be) or Si>5, thus exchange vector (7) does not add Li to the structure. Finally, there is no evidence for a Tschermak-type substitution, i.e., $^{IV}(Mg^{2+},Fe^{2+})+{}^{IV}Si^{4+}={}^{IV}2Al^{3+}$ (5). In summary, the exchange mechanisms (5), (6) and (7), which are known from experiments, cannot be confirmed for the investigated natural cordierites. The same holds for Li entering the channel site: $^{Ch}Li^+ + {}^{VI}Li^+ = {}^{Ch}\square+{}^{VI}Mg^{2+}$ (Kirchner et al., 1984) and $^{Ch}Li^+ + {}^{IV}Al^{3+} = {}^{Ch}\square+{}^{IV}Si^{4+}$ (Schreyer, 1985) do not seem to apply to natural cordierites. The observed discrepancies between natural and experimentally grown cordierites are considered to be mainly due to the restricted range of compositions and P–T conditions accessible to cordierite in the most common natural settings.

We propose a modified general structural formula for natural cordierites, which also considers the incorporation of Mg in the $T_1 1$ site:

$$^{Ch}(Na,K)_{0-1}\,{}^{VI}(Mg,Fe^{2+},Mn,Li)_2\,{}^{IV}Si_5\,{}^{IV}Al_3$$

$$^{IV}(Al,Be,Mg,Fe^{2+},Fe^{3+})O_{18}$$

$$*x^{Ch}(H_2O,CO_2\ldots).$$

For all cordierites with mechanisms (1), (2) and (3) as the dominant mechanisms of coupled substitution, Li and Be contents, if not measured, can be calculated from a mineral formula normalized to 5 Si as Li (a.p.f.u.)=Al+Na−4 and Be (a.p.f.u.)=10−2Al−M^{2+}−Na.

Acknowledgements

We gratefully acknowledge the donors of the cordierite samples listed in Appendix A. The first author would like to thank Charles Geiger for the invitation to the University of Kiel to work on this thrilling topic and for his helpful comments, and L. Ottolini for performing the SIMS analyses. Reviews by Ed Grew, Angelika Kalt and Edward Manning helped to improve the manuscript. This work was supported by DFG, project no. GE 659/6-2.

Appendix A

Lithium and beryllium content of cordierites, expanding on Table 5 of Grew (2002)

Rock type and/or facies and/or mineral assemblage and/or *P–T* estimates, (references)	Locality	Li [ppm] (*n*)	Be [ppm] (*n*)
Pegmatite, vein and unspecified			
Pegmatite (Černý et al., 1997)	Dolní Bory, Czech Republic	497–2560 (8)	4–29 (8)
Pegmatite (Malcherek et al., 2001)	Dolní Bory, Czech Republic	715–725 (2)	0 (2)
Pegmatites (Ginzburg and Stavrov, 1961; Istomin et al., 1997)	Murzinka, Urals, Kazakhstan	883–1998 (3)	19–580 (2)
Pegmatite or possibly vein (miscellaneous) (Istomin et al., 1997)	–	36–1874 (6)	–
Pegmatite (Heinrich, 1950; Newton, 1966; Povondra and Čech, 1978; Armbruster and Irouschek, 1983)	Haddam, CT, USA	1069 (1)	1874–5189 (3)
Nodules in pegmatite (Gordillo et al., 1985)	El Peñón, Argentina	883–976 (5)	3135–4180 (5)
Pegmatite or possibly vein (miscellaneous) (Malcherek et al., 2001)	–	0–534 (9)	0–270 (9)
Metasomatic zones in pegmatite (Černý and Povondra, 1966)	Věžná, Czech Republic	93	6378
Pegmatite (Grew et al., 1995)	Homagama, Sri Lanka	0–9 (3)	0–292
Vein formed by reaction of pegmatitic magma and ultramafic rock (Piyar et al., 1968)	Ukraine (exact locality unknown)	n.a.	6378
Pegmatite (Povondra et al., 1984)	Gammelsmerskärr, Kemiö Island, Finland	n.a.	5585
Metamorphosed pegmatite (Grew et al., 2000; Harley, 1985; Sandiford, 1985)	"Christmas Point", Antarctica	n.a.	3603
Metamorphosed pegmatite (Grew et al., 2000; Harley, 1985; Sandiford, 1985)	Mt. Pardoe, Antarctica	n.a.	2306
Porphyroblast in "bt-cordieritite" a few meters from a pegmatite (Schreyer et al., 1979)	El Pilón, Soto, Argentina	n.a.	3351
Pegmatite (Sambonsugi, 1957; Miyashiro, 1957; Selkregg and Bloss, 1980)	Sugamo, Japan	n.a.	~3600
Pegmatite (Heinrich, 1950; Newton, 1966)	Micanite, CO, USA	n.a.	2522
Pegmatites and veins (Griffitts and Cooley, 1961)	–	n.a.	1.5–2000 (6)
Pegmatite (Newton, 1966)	Bjordammen ("Bjordan"), Bamble, Norway	n.a.	430
Metamorphic			
Miscellaneous metasediments (Ginzburg and Stavrov, 1961)	–	93–2973 (6)	0–144 (6)
Pelitic schist; grt–crd–sil–qtz (Ferry, 1980; Armbruster, 1986, Dutrow et al., 1986)	south-central Maine, USA	3438–4130 (2)	n.a.
Contact metapelite; crd–bt–pl–ilm±grt±and±qtz; *T*=508–762 °C, *P*=2 kbar (Kalt et al., 1998)	Kos, Greece	413–790 (8)	7–22 (8)
Migmatite (Malcherek et al., 2001)	Peña Negra Complex, Spain	534 (1)	22 (1)
Migmatite, (Bea et al., 1994)	Peña Negra Complex, Spain	454–465 (3)	7–16 (3)
Bt-schist and leucocratic ky-gneiss (Armbruster and Irouschek, 1983)	Lepontine Alps, Miregn, Switzerland	0–465 (3)	36 (3)
Micaschist (Armbruster and Irouschek, 1983)	Alpe Sponda, Ticino, Switzerland	232–418 (3)	2162–2919 (3)
Migmatite; crd–bt–grt–pl–kfs–qtz–ilm, 770–846 °C, 4.4–5.1 kbar (Kalt et al., 1999)	Bavarian Forest, Germany	18–133 (–)	1–49 (–)
Cordierite-bearing gneiss (Visser et al., 1994)	Bamble Sector, South Norway	17–115 (20)	<2–257 (20)
Granulite facies; (Grew et al., 1987, 1990)	Ellammankovilpatti, India	37–98 (3)	18–169 (3)

(continued on next page)

Appendix A (*continued*)

Rock type and/or facies and/or mineral assemblage and/or *P–T* estimates, (references)	Locality	Li [ppm] (*n*)	Be [ppm] (*n*)
Granulite facies (miscellaneous) (Grew et al., 1990, 1991)	–	9–42 (5)	0–30 (5)
Sapphirine–cordierite–biotite–garnet–hypersthene rock (Barker, 1964)	Val Codera, Italy	0	5
"Cordieritite" formed by an anatectic process (Schreyer et al., 1979)	El Pilón, Soto, Argentina	n.a.	40–65 (2)
Sil+Kfs zone (Lebedev and Nagaytsev, 1980)	Ladoga complex, NW Russia	n.a.	40 (5)
Hypersthene zone (Lebedev and Nagaytsev, 1980)	Ladoga complex, NW Russia	n.a.	18 (3)
"Kinzigite" (amphibolite-facies metapelite) (Bea and Montero, 1999)	Ivrea-Verbano, Italy	n.a.	12.3
Miscellaneous gneiss (Griffitts and Cooley, 1961)	–	n.a.	10–30 (6)

(*n*): number of analyses; n.a.=not analyzed. Mineral abbreviations after Kretz (1983).

Appendix B

Cordierite sample information

	Sample	Locality and other information	Rock type and/or facies and/or mineral assemblage and/or *P–T* estimates, (references), [donor]
1	TA-2	Haddam, CT, USA	Pegmatite cutting bt-gneiss; crd–qtz–mc–ab–tur–grt–zrn–col–bi–cbrl; (1, 2, 3, 4, 5, 6, 7, 8, 9, 10); [TA]
2	88593	Haddam, Middelsex, CO, USA, 19th Cent	Pegmatite cutting bt–gneiss; crd–qtz–mc–ab–tur–grt–zrn–col–bi–cbrl; (1, 2, 3, 4, 5, 6, 7, 8, 9); [HM]
3	2630	Haddam, CT, USA	Pegmatite cutting bt–gneiss; crd–qtz–mc–ab–tur–grt–zrn–col–bi–cbrl; (1, 2, 3, 4, 5, 6, 7, 8, 9); [SI]
4	84-264-1	Guilford, CT, USA	Pegmatite vein cutting crd–bt–gneiss; (1); [SI]
5	C004	Soendeled, Norway; (8c6b/004)	Pegmatite; qtz–crd; [UKMC]
6	G-155a	Pamirs, Muzkol	Pegmatoid isolations in rock grading from epidote–amphibolite to amphibolite facies. (11); [ES]
7	TUB-1	Dolní Bory, Czech Republic	Pegmatite; sek–ab–ms–qtz–and–srl–bt–crn; (5, 7, 10, 12, 13, 14, 15, 16, 17, 18, 19); [SH]
8	106886	Bjordammen, Bamble, Telemark, Norway	Pegmatite; [HM]
9	TA-4	Arendal, Bamble Sector, S Norway; (#12348)	Granulite facies; bt–crd–grt–amph; 836±49 °C, 7.7±0.3 kbar; (20, 21, 22, 23, 24); [TA]
10	CL-97-2	Lake Cauchon, Manitoba, Canada	Granulite facies; qtz (rt)–kfs–bt–crd–opx–grt–po–zrn; 648 °C/6.1–6.8 kbar; (22); [JKV]
11	VS-1	Chiaravalle, Calabria, Italy; (8/90)	Granulite facies; grt–crd–sil–bt–pl–qtz; 680–790 °C/5.5–7.5 kbar, (25); [VS]
12	VS-2	Colombo, Sri Lanka; (20-4)	Granulite facies; grt–crd–bt–kfs–pl–qtz; 730 °C/5.2–5.9 kbar, (26); [VS]
13	VS-3	Polia, Calabria, Italy (15/81)	Granulite facies; grt–crd–sil–bt–pl–qtz; 680–790±20 °C/5.5–7.5 kbar, (25); [VS]
14	42/IA	Kiranur, South India	Granulite facies; spr–ged–crd–sil–spl–crn–bt–pl; 740±40 °C/7±0.4kbar; (19, 27, 28); [PR]
15	T393	Lhosy, Central Madagascar	Granulite facies; migmatic gneisses; crd–bt–grt±pl±kfs±sil±qtz; 700 °C, 4–5 kbar; (29)
16	40-6	Mt. Ibity, Central Madagascar, Itremo sheet	Amphibolite facies; Metaquartzite; 500–750 °C, 2–6 kbar; (30); [JVK]
17	25Geco mine	GECO mine, Manitouwadge, Ontario, Canada; (HW#1855/44 Crd#25)	Amphibolite facies; crd–po–ccp–py–qtz–bt–fsp; 650±30 °C/6±1 kbar; (22, 31, 32); [JKV]

Appendix B (*continued*)

	Sample	Locality and other information	Rock type and/or facies and/or mineral assemblage and/or *P–T* estimates, (references), [donor]
18	TA-5	Orijärvi, Finland; (#78228)	Orthoamphibole–gneiss; qtz–pl–crd–bt–ilm–ath±ged±cum±alm; 550–600 °C/3 kbar (33); [TA]
19	TA-1	White Well, Western Australia	Phl–schist; crd–crn–phl–tur–sil–rt–zrn; (5, 22, 34, 35, 36) [TA]
20	126178F	Snyder Bay, Canada	Contact aureole; 450–900 °C, 2.25 kbar (5, 7, 37, 38)
21	C005	Sundsvall, Sweden; (8c6b/005)	Migmatic schist; crd–bt–qtz–pl–grt; [UKMC]
22	WYO-2	Laramie Range, Albany, WY, (Laramie Range cordierite no.2), USA	Metasomatic cordierite—deposit in a metamorphosed norite; (22,39,40); [JKV]
23	118871	Richmond, Cheshire, NH (Harris soapstone quarry?) USA	Quartz–vein; crd–qtz–tur–rt; qtz–crd–(ky)–crn–st–ath; (41); [HM]
24	HO6	El Joyazo volcano (Cerro de Joyazo), SE Spain	Metapelitic xenolithes in dacitic lava; loose crystal; 850±50 °C, 5–7 kbar; (42); [BC]
25	CTsiM	Tsihombe, South Madagascar	Granulite facies; [SH]
26	C006	Madagascar; (8c6b/006)	Granulite facies; [UKMC]
27	129875	Manik Ganga, Sri Lanka	Granulite facies; [HM]
28	7114	Sopparjok, Norway	Crd–grt–gneiss; [UKMC]
29	7107	Airport Ivalo, Finland	Crd–grt–gneiss; [UKMC]
30	TA-6	Hards Range, Australia	(22); [TA]
31	TA-3	Tanzania	Gemstone; [TA]
32	C2623	Tanzania	Gemstone [HM]
33	DA-1	Zimbabwe	Gemstone; [DA]
34	CMikM	Mikon, Madagascar	

Mineral abbreviations: albite (ab), almandine (alm), amphibole (amph), andalusite (and), anthophyllite (ath), bismutite (bi), biotite (bt), chalcopyrite (ccp), chrysoberyl (cbrl), columbite (col), cordierite (crd), corundum (crn), cummingtonite (cum), garnet (grt), gedrite (ged), ilmenite (ilm), K-feldspar (kfs), kyanite (ky), microcline (mc), muscovite (ms), orthopyroxene (opx), phlogopite (phl), plagioclase (pl), pyrite (py), pyrrhotite (po), quartz (qtz), rutile (rt), sapphirine (spr), schorl (srl), sekaninaite (sek), sillimanite (sil), spinel (spl), staurolite (st), tourmaline (tur), zircon (zrn).

References: (1) Heinrich (1950), (2) Miyashiro (1957), (3) Leake (1960), (4) Newton (1966), (5) Goldman et al. (1977), (6) Povondra and Čech (1978), (7) Selkregg and Bloss (1980), (8) Armbruster and Irouschek (1983), (9) Armbruster (1986), (10) Kolesov and Geiger (2000), (11) Istomin et al. (1997), (12) Sekanina (1928), (13) Stanek and Miškovský (1964), (14) Stanek and Miškovský (1975), (15) Nemec (1976), (16) Schreyer et al. (1993), (17) Černý et al. (1997), (18) Malcherek et al. (2001), (19) Geiger et al. (2000a), (20) Lamb et al. (1986), (21) Petersen and Vally (1988), (22) Vry et al. (1990), (23) Nijland and Maijer (1993), (24) Visser et al. (1994), (25) Schenk (1989), (26) Raase and Schenk (1994), (27) Lal et al. (1984), (28) Geiger et al. (2000b), (29) Nicollet (1990), (30) Morteani et al. (in review), (31) James et al. (1978), (32) Petersen and Essene (1982), (33) Schneiderman and Tracy (1991), (34) Pryce (1973), (35) Armbruster and Bloss (1980), (36) Armbruster (1985a), (37) Speer (1978), (38) Speer (1982), (39) Newhouse and Hagener (1949), (40) Iiyima (1960), (41) Robinson and Jaffe (1969), (42) Cesare et al. (1997).

Donors: T. Armbruster [TA], Harvard Museum [HM], Smithsonian Institution: National Museum of Natural History [SI], University of Kiel Mineral collection [UKMC], E. Sokol [ES], S. Hertig [SH], J.K. Vry [JKV], V. Schenk [VS], P. Raase [PR], B. Cesare [BC], D. Akermand [DA].

References

Armbruster, T., 1985a. Ar, N_2 and CO_2 in the structural cavities of cordierite, an optical and X-ray single crystal study. Phys. Chem. Miner. 12, 233–245.

Armbruster, T., 1985b. Fe-rich cordierites from acid volcanic rocks: an optical and X-ray single-crystal structure study. Contrib. Mineral. Petrol. 91, 180–187.

Armbruster, T., 1986. Role of Na in the structure of low-cordierite: a single-crystal X-ray study. Am. Mineral. 71, 746–757.

Armbruster, T., Bloss, F.D., 1980. Channel CO_2 in cordierites. Nature 286, 140–141.

Armbruster, T., Irouschek, A., 1983. Cordierites from the Lepontine Alps: Na+Be→Al substitution, gas content, cell parameters and optics. Contrib. Mineral. Petrol. 82, 389–396.

Barker, F., 1964. Reaction between mafic magmas and pelitic schists, Cortland, New York. Am. J. Sci. 262, 614–634.

Bea, F., 1996. Residence of REE, Y, Th and U in granites and crustal protoliths: implications for the chemistry of crustal melts. J. Petrol. 37, 521–552.

Bea, F., Montero, P., 1999. Behavior of accessory phases and redistribution of Zr, REE, Y, Th and U during metamorphism and partial melting of metapelites in the lower crust: an example from the Kinzigite Formation of Ivrea-Verbano, NW Italy,. Geochim. Cosmochim. Acta 63, 1133–1153.

Bea, F., Pereira, M.D., Stroh, A., 1994. Mineral/leucosome trace-element partitioning in a peraluminous migmatite a laser ablation-ICP-MS study. Chem. Geol. 117, 291–312.

Bea, F., Montero, P., Stroh, A., Baasner, J., 1996. Microanalyses of minerals by an excimer UV-LA-ICP-MS system. Chem. Geol. 133, 145–156.

Beeson, R., 1978. The geochemistry of orthoamphiboles and coexisting cordierites and phlogopites from South Norway. Contrib. Mineral. Petrol. 66, 5–14.

Behrens, H., Stuke, A., 2003. Quantification of H_2O contents in silicate glasses using IR spectroscopy—a calibration based on hydrous glasses analysed by Karl–Fischer titration. Glass Sci. Technol. (submitted for publication).

Behrens, H., Romano, C., Nowak, M., Holtz, F., Dingwell, D.B., 1996. Near-infrared spectroscopic determination of water species in glasses of the system $MAlSi_3O_8$ M=Li,Na, K. An interlaboratory study. Chem. Geol. 128, 41–64.

Behrens, H., Tamic, N., Holtz, F., 2003. Determination of molar absorption coefficient for the IR absorption band of CO_2 in rhyolitic glasses. Am. Mineral. (submitted for publication).

Beltrame, R.J., Norman, D.I., Alexander, E.C., Sawkins, F.J., 1976. Volatiles released by step-heating a cordierite to 1200 °C. Trans. Am. Geophys. Union 57, 352.

Černý, P., 2002. Mineralogy of beryllium in granitic pegmatites. In: Grew, E.S. (Ed.), Beryllium: Mineralogy, Petrology and Geochemistry, Rev. Mineral. Geochem., vol. 50, pp. 405–444.

Černý, P., Povondra, P., 1966. Beryllian cordierite from Věžná Na, K.+Be→Al, N. Jahrb. Mineral., Monatsh. 44, 36–44.

Černý, P., Chapman, R., Schreyer, W., Ottolini, L., Bottazzi, P., McCammon, C.A., 1997. Lithium in sekaninaite from the type locality, Dolní Bory, Czech Republic. Can. Mineral. 35, 167–173.

Cesare, B., Mariani, E.S., Venturelli, G., 1997. Crustal anatexis and melt extraction during deformation in restitic xenoliths at El Joyazo. Mineral. Mag. 61, 15–27.

Cohen, J.P., Ross, F.K., Gibbs, G.V., 1977. An X-ray and neutron diffraction study of hydrous low cordierite. Am. Mineral. 62, 67–78.

Damon, P.E., Kulp, J.L., 1958. Excess helium and argon in beryl and other minerals. Am. Mineral. 43, 433–459.

Dutrow, B.L., Holdaway, M.J., Hinton, R.W., 1986. Lithium in staurolite and its petrologic significance. Contrib. Mineral. Petrol. 94, 496–506.

Evans, D.L., Fisher, G.R., Geiger, J.E., Martin, F.W., 1980. Thermal expansions and chemical modifications of cordierite. J. Am. Ceram. Soc. 63, 629–634.

Evensen, J.M., London, D., 2002. Experimental silicate mineral/melt partition coefficients for beryllium and the crustal Be cycle from migmatite to pegmatite. Geochim. Cosmochim. Acta 66, 2239–2265.

Evensen, J.M., London, D., 2003. Experimental partitioning of Be, Cs, and other trace elements between cordierite and felsic melt, and the chemical signature of S-type granite. Contrib. Mineral. Petrol. 144, 739–757.

Faye, G.H., Manning, P.G., Nickel, E.H., 1968. An interpretation of the polarized optical absorption spectra of tourmaline, cordierite, chloritoide and vivianite. Am. Mineral. 53, 1174–1201.

Fermor, L.L., 1924. Discussion of Tilley CE Contact metamorphism in Comrie Area of the of the Perthshire Highland. Q. J. Geol. Soc. 80, 629–634.

Ferry, J.M., 1980. A comparative study of geothermometers and geobarometers in pelitic schists from south central Maine. Am. Mineral. 65, 720–732.

Garbe-Schönberg, C.D., 1993. Simultaneous determination of 37 trace elements in 28 international rock standards by ICP-MS. Geostand. Newsl. 17, 81–93.

Geiger, C.A., Armbruster, T., Khomenko, V., Quartieri, S., 2000a. Cordierite: I. The coordination of Fe^{2+}. Am. Mineral. 85, 1255–1264.

Geiger, C.A., Rager, H., Czank, M., 2000b. Cordierite: III. The site occupation and concentration of Fe^{3+}. Contrib. Mineral. Petrol. 140, 344–352.

Gibbs, G.V., 1966. The polymorphism of cordierite: I. The crystal structure of low cordierite. Am. Mineral. 51, 1068–1087.

Ginzburg, A.I., Stavrov, O.D., 1961. Content of rare elements in cordierite. Geochemistry 1961, 208–211.

Giraud, A., Dupuy, C., Dostal, J., 1986. Behaviour of trace elements during magmatic processes in the crust. Application to acidic volcanic rocks of Tuscany Italy. Chem. Geol. 57, 269–288.

Goldman, R.S., Rossman, G.R., Dollase, W.A., 1977. Channel constituents in cordierite. Am. Mineral. 62, 1144–1157.

Gordillo, C.E., Schreyer, W., Werding, G., Abraham, K., 1985. Lithium in NaBe-cordierites from El Peñón, Sierra de Córdoba, Argentina. Contrib. Mineral. Petrol. 90, 93–101.

Grew, E.S., 2002. Beryllium in metamorphic environments (emphasis on aluminous compositions). In: Grew, E.S. (Ed.), Beryllium: Mineralogy, Petrology and Geochemistry, Rev. Mineral. Geochem., vol. 50, pp. 487–549.

Grew, E.S., Abraham, K., Medenbach, O., 1987. Ti-poor hoegbomite in kornerupine–cordierite–sillimanite rocks from Ellammankovilpatti, Tamil Nadu, India. Contrib. Mineral. Petrol. 95, 21–31.

Grew, E.S., Chernosky, J.V., Werding, G., Abraham, K., Marquez, N., Hinthorne, J.R., 1990. Chemistry of kornerupine and associated minerals, a wet chemical, ion microprobe, and X-ray study emphasizing Li, Be, B and F contents. J. Petrol. 31, 1025–1070.

Grew, E.S., Yates, M.G., Beryozkin, V.I., Kitsul, V.I., 1991. Kornerupine in slyudites from the Usmun River Basin in the Aldan Shield: Part II. Chemistry of the minerals, mineral reactions. Sov. Geol. Geophys. 32, 85–98.

Grew, E.S., Hiroi, Y., Motoyoshi, Y., Kondo, Y., Jayatileke, S.J.M., Marquez, N., 1995. Iron-rich kornerupine in sheared pegmatite from the Wanni Complex, at Homagama, Sri Lanka. Eur. J., 7623–7636.

Grew, E.S., Yates, M.G., Barbier, J., Shearer, C.K., Sheraton, J.W., Shiraishi, K., Motoyoshi, Y., 2000. Granulite-facies beryllium pegmatites in the Napier Complex in Khmara and Amundsen Bays, western Enderby Land, East Antarctica. Polar Geosci. 13, 1–40.

Griffitts, W.R., Cooley, E.F., 1961. Beryllium content of cordierite. U. S. Geol. Surv. Prof. Pap. 424-B, 259.

Harley, S.L., 1985. Paragenetic and mineral–chemical relationships in orthoamphibole-bearing gneisses from Enderby Land, east

Antarctica a record of Proterozoic uplift. J. Metamorph. Geol. 3, 179–200.

Harris, N.B.W., Gravestock, P., Inger, S., 1992. Ion-microprobe determinations of trace-element concentrations in garnets from anatectic assemblage. Chem. Geol. 100, 41–49.

Heinrich, E.W., 1950. Cordierite in pegmatite near Micanite, Colorado. Am. Mineral. 35, 173–184.

Hentschel, G., 1977. Neufunde seltener Minerale im Laacher Vulkangebiet. Aufschlusβ 28, 129–133.

Hochella, M.F., Brown, G.E., Ross, F.K., Gibbs, G.V., 1979. High-temperature crystal chemistry of hydrous Mg-and Fe-cordierites. Am. Mineral. 64, 337–351.

Hölscher, A., Schreyer, W., Lattard, D., 1986. High-pressure, high-temperature stability of surinamite in the system $MgO–BeO–Al_2O_3–SiO_2–H_2O$. Contrib. Mineral. Petrol. 92, 113–127.

Iiyima, T., 1955. Existence of indialite solid solutions. Proc. Imp. Acad. Jpn. 32, 166–168.

Iiyima, T., 1960. Recherches sur le rôle de l'eau dans la structure et le polymorphism de la cordiérite. Bull. Soc. Fr. Minéral. Cristallogr. 83, 511–514.

Istomin, V.E., Sokol, E.V., Lepezin, G.G., 1997. Blocks within crystal structure and peculiarities of behaviour of Mn^{2+} and Fe^{2+} in cordierite. Russ. Geol. Geophys. 38, 825–831.

James, R., Grieve, R.A.F., Pauk, L., 1978. The petrology of cordierite–anthophyllite–gneisses and associated mafic and pelitic gneisses, Manitowadge, Ontario. Am. J. Sci. 278, 41–63.

Jarosewich, E., Nelen, J.A., Norberg, J.A., 1980. Reference samples for electron microprobe analysis. Geostand. Newsl. 4, 43–47.

Kalt, A., Altherr, R., Ludwig, T., 1998. Contact metamorphism in pelitic rocks on the island of Kos Greece, Eastern Aegean Sea. A test fort the Na-in-cordierite thermometer. J. Petrol. 39, 663–688.

Kalt, A., Berger, A., Blümel, P., 1999. Metamorphic evolution of cordierite-bearing migmatites from the Bayerischer Wald Variscan Belt, Germany. J. Petrol. 40, 601–627.

Kirchner, D., Mirwald, P.W., Schreyer, W., 1984. Experimenteller Li-Einbau in Mg-Cordierit. Fortschr. Mineral. 62, 119–120.

Klaska, R., Grew, E.S., 1991. The crystal structure of B-free kornerupine: conditions favoring the incorporation of variable amounts of B through $^{[4]}B \Leftrightarrow {}^{[4]}Si$ substitution in kornerupine. Am. Mineral. 76, 1824–1835.

Koch-Müller, M., Langer, K., Behrens, H., Schuck, G., 1997. Crystal chemistry and infrared spectroscopy in the OH-stretching region of synthetic staurolites. Eur. J. Mineral. 9, 67–82.

Kolesov, B.A., Geiger, C.A., 2000. Cordierite: II. The role of CO_2 and H_2O. Am. Mineral. 85, 1265–1274.

Kretz, R., 1983. Symbols for rock-forming minerals. Am. Mineral. 68, 277–279.

Lal, R.K., Akermand, D., Raith, M., Raase, P., Seifert, F., 1984. Sapphirine-bearing assemblages from Kiranur, Southern India. A study of chemographic relationships in the $Na_2O–FeO–MgO–Al_2O_3–SiO_2–H_2O$ system. Neues Jahrb. Mineral. 150, 121–152.

Lamb, R.C., Smalley, P.C., Field, D., 1986. *P–T* conditions for the Arendal granulites, southern Norway implications for the roles of *P*, *T* and CO_2 in deep crustal LILE depletion. J. Metamorph. Geol. 4, 143–160.

Leake, B.E., 1960. Compilation of chemical analyses and physical constants of natural cordierites. Am. Mineral. 45, 282–298.

Lebedev, V.I., Nagaytsev, Y.V., 1980. Minor elements in metamorphic rocks as an ore material source for certain deposits. Geochem. Int. 17, 31–39.

London, D., 1995. Geochemical features of peraluminous granites, pegmatites and rhyolites as sources of lithophile metal deposits. Mineral. Assoc. Can., Short Course Handb. 23, 175–202.

London, D., Evensen, J.M., 2002. Beryllium in silicic magmas and the origin of beryl-bearing pegmatites. In: Grew, E.S. (Ed.), Beryllium: Mineralogy, Petrology, and Geochemistry, Mineral. Soc. Am. Rev. Mineral Geochem., vol. 50, pp. 445–486.

Malcherek, T., Domeneghetti, M.C., Tazzoli, V., Ottolini, L., McCammon, C., Carpenter, M.A., 2001. Structural properties of ferromagnesian cordierites. Am. Mineral. 86, 66–79.

Meagher, E.P. (1967). The crystal structure and polymorphism of cordierite. PhD thesis. Pennsylvania State University, University Park.

Meagher, E.P., Gibbs, G.V., 1977. The polymorphism of cordierite: II. The crystal structure of Indialite. Can. Mineral. 15, 43–49.

Miyashiro, A., 1957. Cordierite–indialite relations. Am. J. Sci. 255, 43–62.

Miyashiro, A., Iiyama, T., 1954. A preliminary note on a new mineral, indialite, polymorphic with cordierite. Proc. Jpn. Acad. 30 (8), 746–751.

Morteani, G., Razakamanana, T., Akermand, D., 2003. The lazulite–tourmaline–dumortierite-bearing metaquartzites of the Mesoproterozoic Itrema sheet, Central Madagascar geochemistry. Mineral. Petrol. (in review).

Mottana, A., Fusi, A., Potenza, B.B., Crespi, R., Liborio, G., 1983. Hydrocarbon-bearing cordierite from the Derivo-Coloico road tunnel Como, Italy. Neues Jahrb. Mineral., Geol. Paläontol., Abh. 148, 181–199.

Němec, J., 1976. Versuch einer paragenetischen Analyse der Pegmatite Böhmens und Mährens. An Attempt of the Paragenetic Analyses of Pegmatites from Bohemia and Morovia. Chem. Erde 35, 126–157.

Newhouse, W.H., Hagener, A.F., 1949. Cordierite deposits of the Laramie Range, Albany County, Wyoming. Geol. Survey Bull., Wyoming 41.

Newton, R.C., 1966. BeO in pegmatitic cordierite. Min. Mag. 35, 920–927.

Nicollet, C., 1990. Occurrences of grandidierite, serendibite and tourmaline near Ihousy, southern Madagascar. Mineral. Mag. 54, 131–133.

Nijland, T.G., Maijer, C., 1993. The regional amphibolite to granulite facies transition at Arendal, Norway. Evidence for a thermal dome. Neues Jahrb. Abh. 165, 191–221.

Ottolini, L., Bottazzi, P., Vannucci, R., 1993. Quantification of lithium, beryllium and boron in silicates by secondary ion mass spectrometry using conventional energy filtering. Anal. Chem. 65, 1960–1968.

Parkin, K.M., Loeffler, B.M., Burns, R.G., 1977. Mössbauer spectra of kyanite, aquamarine and cordierite showing intervalence charge transfer. Phys. Chem. Miner. 1, 301–311.

Petersen, D.E., Vally, J.W., 1988. Comparison of ideal and non-ideal orthopyroxene activities in Alm-Fs and Py-En geobarometry. Abstr. Programs - Geol. Soc. Am. 20, A98.

Petersen, E.U., Essene, E.J., 1982. Metamorphism of the Gecco massive sulfide deposit, Manitowadge, Ontario. Abstr. Programs - Geol. Ass. Can. Mineral. Ass. Can., 73.

Piyar, U.K., Gorshnikov, B.I., Yur'yev, L.D., 1968. Be-cordierite from metamorphic rocks of Ukraine. Mineral. Sb. (L'vov) 22, 86.

Pollack, H., 1976. Charge transfer in cordierite. Phys. Status Solidi, B Basic Res. 74, 31–34.

Povondra, P., Čech, F., 1978. Sodium–beryllium-bearing cordierite from Haddam, Connecticut, U.S.A. Neues Jahrb. Mineral., Monatsh. 5, 203–209.

Povondra, P., Čech, F., Burke, E.A.J., 1984. Sodian–beryllian cordierite from Gammelmorskärr, Kemiö Island, Finland and its decomposition products. Neues Jahrb. Mineral., Monatsh. 1984, 125–136.

Pryce, M.W., 1973. Low-iron cordierite from phlogopite schist White Well, Western Australia. Mineral. Mag. 39, 241–243.

Raase, P., Schenk, V., 1994. Petrology of granulite-facies metapelites of the Highland Complex, Sri Lanka. Implications for the metamorphic zonation and the *P–T* path. Precambrian Res. 66, 265–294.

Robbins, D.W., Sterns, R.G.J., 1968. Polarization-dependence and oscillator strength of metal–metal charge-transfer bands in iron (II, III) silicate minerals. Chem. Commun. 4, 508–509.

Robinson, P., Jaffe, H.W., 1969. Aluminous enclaves in gedrite–cordierite gneiss from southwestern New Hampshire. Am. J. Sci. 267, 389–421.

Sambonsugi, M., 1957. Iron-rich cordierite structurally close to indialite. Proc. Jpn. Acad. 33, 190–195.

Sandiford, M., 1985. The origin of retrograde shear zones in the Napier Complex implications for the tectonic evolution of Enderby Land, Antarctica. J. Struct. Geol. 7, 477–488.

Schenk, V., 1989. *P–T–t* path of the lower crust in the hercynian belt of southern Calabria. In: Daly, J.S., Cliff, R.A., Yardly, B.W.D. (Eds.), Evolution of Metamorphic Belts, Geol. Soc. Special Publications, vol. 43, pp. 337–342.

Schneiderman, J.S., Tracy, R.J., 1991. Petrology of orthoamphibole–cordierite gneisses from the Orijärvi area, SW Finland. Am. Mineral. 76, 942–955.

Schreyer, W., 1965. Synthetische und natürliche Cordierite I Mischkristallbildung synthetischer Cordierite und ihre Gleichgewichtsbeziehungen. Neues Jahrb. Mineral. 103, 35–79.

Schreyer, W., 1985. Experimental studies on cation substitutions and fluid incorporation in cordierite. Bull. Minéral. 108, 273–291.

Schreyer, W., Schairer, F.J., 1961. Compositions and structural states of anhydrous Mg-cordierites a reinvestigation of the central part of the system $MgO–Al_2O_3–SiO_2$. J. Petrol. 2, 324–406.

Schreyer, W., Yoder, H.S., 1964. The system Mg-cordierite–H_2O and related rocks. Neues Jahrb. Mineral. 101, 271–342.

Schreyer, W., Gordillo, C.E., Werding, G., 1979. A new sodian–beryllian cordierite from Soto, Argentina, and the relationship between distortion index, Be content, and state of hydration. Contrib. Mineral. Petrol. 70, 421–428.

Schreyer, W., Maresch, W.V., Daniels, P., Wolfsdorff, P., 1990. Potassic cordierites characteristic minerals for high-temperature, very low pressure environments. Contrib. Mineral. Petrol. 105, 162–172.

Schreyer, W., Bernhard, H.J., Medenbach, O., 1993. Ferrogedrite, siderophyllite, septachamosite, andalusite and chloritoid as alteration products of sekaninaite ferrocordierite from Dolní Bory pegmatite, Moravia. Geol. Geofiz. 34, 141–147 (in Russ.).

Sekanina, J., 1928. Minerals of Moravian pegmatites. Acta Mus. Morav., Sci. Nat. 26, 113–224 (in Czech).

Selkregg, K.R., Bloss, F.D., 1980. Cordierites compositional controls of Δ, cell parameters and optical properties. Am. Mineral. 65, 522–533.

Smart, R.M., Glasser, F.P., 1977. Stable cordierite solid solutions in the $MgO–Al_2O_3–SiO_2$ system composition, polymorphism and thermal expansion. Sci. Ceram. 9, 256–263.

Smith, G., Strens, R.G.J., 1976. Intervalence transfer absorption in some silicate, oxide and phosphate minerals. In: Sterns, R.G.J. (Ed.), The Physics and Chemistry of Minerals and Rocks. Wiley, New York, pp. 583–612.

Sokol, E., Volkova, N., Lepezin, G., 1998. Mineralogy of pyrometamorphic rocks associated with naturally burned coal-bearing spoil-heaps of the Chelyabinsk coal basin, Russia. Eur. J. Mineral. 10, 1003–1014.

Speer, J.A., 1978. The stratigraphy and depositional environment of the Aphebian Snyder Group, Labrador. Can. J. Earth Sci. 15, 52–68.

Speer, J.A., 1982. Metamorphism of the pelitic rocks of the Snyder Group in the contact aureole of the Kiglapait layered intrusion. Labrador Effects of buffering partial pressures of water. Can. J. Earth Sci. 19, 1888–1909.

Staněk, J., Miškovský, J., 1964. Iron-rich cordierite from the Dolní Bory pegmatite. Čas. Mineral. Geol. 9, 191–192 (in Czech).

Staněk, J., Miškovský, J., 1975. Sekaninaite, a new mineral of the cordierite series, from Dolní Bory, Czechoslovakia. Scr. Fac. Sci. Nat. UJEP Brun., Geol. 15, 21–30.

Steppan, N. (2003). Li, Be und B in Mineralen metapelitischer Gesteine: Fallstudien auf der Insel Ikaria, im künischen Gebirge und den Schweizer Alpen. Inaugural-Dissertation, Ruprecht-Karls-Universität Heidelberg. http://archiv.ub.uni-heidelberg.de/volltextserver/volltexte/2004/4283/pdf/nsteppan.pdf.

Thompson, P., Harley, S.L., Carrington, D.P., 2002. Sodium and potassium in cordierite—a potential thermometer for melts? Eur. J. Mineral. 14, 459–470.

Vance, E.R., Price, D.C., 1984. Heating and radiation effects on optical and Mössbauer spectra of Fe-bearing cordierites. Phys. Chem. Miner. 23, 391–401.

Venkatesh, V., 1952. Development and growth of cordierite in paralavas. Am. Mineral. 37, 831–848.

Visser, D., Kloprogge, J.T., Maijer, C., 1994. An infrared spectroscopic IR and light element Li, Be, Na. Study of cordierites from the Bamble Sector, South Norway. Lithos 32, 95–107.

Vry, K.J., Brown, P.E., Valley, J.W., 1990. Cordierite volatile content and the role of CO_2 in high grade metamorphism. Am. Mineral. 75, 71–88.

Wallace, J.H., Wenk, H.R., 1980. Structure variations in low cordierites. Am. Mineral. 65, 96–111.

Wolfsdorff, P., Schreyer, W., 1992. Synthesis of sodian cordierites in the system Na_2O–MgO–Al_2O_3–SiO_2. Neues Jahrb. Mineral., Geol. Paläontol., Monatsh. 2, 80–96.